nature communications

Article

https://doi.org/10.1038/s41467-025-59850-8

G_zESTY as an optimized cell-based assay for initial steps in GPCR deorphanization

Received: 26 July 2024

Accepted: 6 May 2025

Published online: 15 May 2025

Check for updates

Luca Franchini, Joseph J. Porter, John D. Lueck & Cesare Orlandi

G protein-coupled receptors (GPCRs) are key pharmacological targets, yet many remain underutilized due to unknown activation mechanisms and ligands. Orphan GPCRs, lacking identified natural ligands, are a high priority for research, as identifying their ligands will aid in understanding their functions and potential as drug targets. Most GPCRs, including orphans, couple to $G_{i/o/z}$ family members, however current assays to detect their activation are limited, hindering ligand identification efforts. We introduce G_zESTY, a sensitive, cell-based assay developed in an easily deliverable format designed to study the pharmacology of $G_{i/o/z}$-coupled GPCRs and assist in deorphanization. We optimized assay conditions and developed an all-in-one vector employing cloning methods to ensure the correct expression ratio of G_zESTY components. G_zESTY successfully assessed activation of a library of ligand-activated GPCRs, detecting both full and partial agonism, and responses from endogenous GPCRs. Notably, with G_zESTY we established the presence of endogenous ligands for GPR176 and GPR37 in brain extracts, validating its use in deorphanization efforts. This assay enhances the ability to find ligands for orphan GPCRs, expanding the toolkit for GPCR pharmacologists.

In mammals, G Protein Coupled Receptors (GPCRs) are the largest family of cell surface receptors and are involved in a wide range of physiological and pathological processes[1,2]. Orphan GPCRs are those whose natural ligands have not yet been identified or agreed upon, making them difficult to study. Deorphanization, the process of identifying endogenous ligands for orphan GPCRs, is often achieved by analyzing receptor activation by candidate ligands in heterologous cell systems. These candidate ligands are selected based on their overlapping in vivo localization with a target GPCR, by isolation from tissue extracts that exert measurable physiological effects, or via screening of large libraries of endogenous compounds including small molecules, peptides, and lipids with a demonstrated biological activity[3–11]. Research that led to the deorphanization of the Glucagon-Like Peptide-1 (GLP1) receptor illustrates how identifying a GPCR's endogenous ligand can unlock new therapeutic opportunities. Initially discovered as a gut-derived hormone that enhances insulin secretion in response to elevated plasma glucose levels[12], GLP1 was found to bind to a putative receptor in the brain and pancreas[13,14]. This discovery led to the cloning of its receptor, a GPCR, in the early 1990s[15–17]. Since then, numerous GLP1 receptor agonists have been approved for treating type 2 diabetes mellitus and, more recently, for chronic weight management in adults with obesity[18–20].

A central challenge in the process of deorphanization is the choice of a measurable outcome of receptor activation. Cell-based assays exploiting various signaling properties and readouts have been developed, each with their own advantages and limitations. These assays measure proximal events such as heterotrimeric G protein dissociation[21–24] or β-arrestin recruitment[25,26]; they quantify the accumulation of second messengers[27–30]; or they utilize genetic reporters that depend on transcriptional regulation events initiated by GPCRs[31,32]. Further sets of assays are label-free and agnostic to the molecular mechanism leading to the change being measured[33,34]. All of these assays differ in sensitivity and time required to obtain a measurable signal. Most importantly, when studying orphan GPCRs, lack of information about G protein coupling profile or ability to recruit β-arrestins requires further considerations. To partially address this

Department of Pharmacology and Physiology, University of Rochester Medical Center, Rochester, NY 14642, USA.
e-mail: cesare_orlandi@urmc.rochester.edu

issue, we recently quantified the constitutive activity of several orphan GPCRs and showed that many are coupled to G proteins belonging to the $G_{i/o/z}$ family[35].

Here, we performed an in-depth optimization of a cell-based assay aimed at measuring $G_{i/o/z}$ coupled receptor activation. We demonstrated an improved sensitivity and the wide applicability of this assay that we named G_z Enhanced Signal Transduction assaY (G_zESTY). We generated and tested an all-in-one plasmid for the mammalian expression of each component required for G_zESTY at the optimized ratio. Finally, we applied this assay to demonstrate the presence of endogenous ligands for orphan receptors GPR176 and GPR37 in unfractionated mouse brain extract.

Results

G_s-based protein chimeras combined with a cAMP biosensor allow for the measurement of the activation of $G_{i/o/z}$-coupled receptors

Several cell-based assays are currently available to study the activation of $G_{i/o/z}$-coupled receptors. In the G protein nanoBRET assay, receptor activation in response to ligands is measured as an increase in BRET signal due to the release of Gβγ-venus and its interaction with a membrane-anchored biosensor that consists of the C-terminus of GRK3 fused to Nluc (Supplementary Fig. 1A)[22,35]. The main advantage of this assay is the rapid measurement of a proximal event in GPCR activation that allows for real-time analysis of the receptor kinetics but with a trade-off in assay sensitivity (Supplementary Fig. 1D). Genetic reporters expressing luciferase under the control of a GPCR-inducible promoter are commonly used. These assays have been developed to detect signals downstream of GPCR coupling to G_s (CRE-luc reporter), G_q (NFAT-luc reporter), and $G_{12/13}$ (SRE-luc reporter)[32]. Activation of $G_{i/o/z}$-coupled receptors can be quantified as a reduction in the luciferase accumulation using a CRE-luc reporter, or indirectly as Gβγ modulation of signaling pathways regulating the SRE-luc reporter. A more sensitive approach adopts G protein chimeras based on the core of $G\alpha_s$ or $G\alpha_q$ and the last few amino acids of members of the $G_{i/o/z}$ family[36,37]. This strategy allows the detection of an accumulation of luciferase using CRE-luc and NFAT-luc, respectively, in response to the activation of $G_{i/o/z}$-coupled receptors (Supplementary Fig. 1B). One limitation of this approach is that the receptor must be exposed to an agonist for an extended time to accumulate measurable quantities of luciferase in the cell (Supplementary Fig. 1D). During this time, processes like receptor desensitization, internalization, and compensatory mechanisms can take place in the cell reducing the assay reliability. A good compromise between speed and assay sensitivity is based on measuring the accumulation of second messengers. Activation of $G_{i/o/z}$-coupled receptors inhibits the activity of adenylyl cyclase thereby reducing cAMP accumulation in response to forskolin treatments. Real-time measurements of cAMP levels can rapidly indicate if a $G_{i/o/z}$-coupled receptor has been activated. This assay depends on the side-by-side comparison of cAMP accumulation in cells treated with an agonist and in cells treated with vehicle. Such an approach is rapid, achieving a signal plateau within 15 min of agonist application (Supplementary Fig. 1C, D). Alternatively, co-expression of $G\alpha_s$-based chimeras bearing the C-terminus of $G_{i/o/z}$ family members can be used to redirect receptor activation to stimulate adenylyl cyclase and cAMP accumulation (Supplementary Fig. 1C, D)[27]. Overall, this last strategy yields an optimal balance between assay duration and sensitivity.

Building on these observations, we tested the activation of four prototypical $G_{i/o/z}$-coupled GPCRs, dopamine D2 receptor (D2R), α2 adrenergic receptor (ADRA2A), γ-aminobutyric acid B receptor (GABAB), and μ opioid receptor (MOR) using three $G\alpha_s$-based chimeras bearing the C-terminus of $G\alpha_i$, $G\alpha_o$, and $G\alpha_z$. Application of selective agonists revealed a robust accumulation of intracellular cAMP as measured using a split-luciferase GloSensor (Fig. 1A). We measured baseline luminescence for 3 min before applying each agonist as well as the maximal amplitude obtained in response to agonist stimulation (Fig. 1B). Using these measurements, we calculated the fold change induction for each condition as an index that we can use to compare sensitivity between assays (Fig. 1C). These experiments revealed that all three $G\alpha_s$-based chimeras are effective tools for detecting the activation of $G_{i/o/z}$-coupled receptors as an increased intracellular accumulation of cAMP. Moreover, two out of four GPCR tested exhibited a significantly higher fold change when the GsGz chimera was co-transfected, likely due to a lower baseline level.

The assay sensitivity shows a clear dependence on both the transfection ratio of assay components and the inhibition of endogenous $G_{i/o}$ proteins

We optimized the assay conditions by adjusting the amount of transfected plasmids used to express each $G\alpha_s$-chimera. (Fig. 2A). We found that, generally, excessive amounts of $G\alpha_s$-chimeras result in higher baselines, which attenuate the observed fold change (Supplementary Fig. 2). Moreover, considering that GsGz, just like $G\alpha_z$, is insensitive to the action of pertussis toxin (PTX), we introduced it in the assay aiming to reduce the adenylyl cyclase inhibition due to endogenous $G\alpha_{i/o}$ proteins. We found that very low levels of transfected PTX boosted the induction of cAMP for each GPCR from a minimum of 1.5 times (GABABR) to a maximum of 6.1 times (D2R) (Fig. 2B; Supplementary Fig. 3). Similarly, keeping a fixed amount of PTX, we titrated the amount of the GsGz chimera. We observed comparable effects with each of the four receptors indicating an optimal amount of GsGz at 45–138 ng over a total of 2.5 μg of transfected DNA (Fig. 2C; Supplementary Fig. 4). Finally, we observed that the greatest accumulation of cAMP was achieved when transfecting the highest amount of receptor (Fig. 2D; Supplementary Fig. 5). Based on these results, we recalibrated the amount of each transfected plasmid, expressing the four assay components, and determined the optimal conditions as a molar ratio of 50:47.5:1.8:0.7 (GloSensor:GPCR:GsGz:PTX) (Fig. 2E). These optimization steps led to an overall 3–6 fold improvement in assay sensitivity measured as a fold change accumulation in cAMP. Given that HEK293 cells express $G\alpha_z$[38], we explored if transfecting cells with the catalytic subunit of OZITX instead of PTX would further boost the signal because it inhibits each $G_{i/o/z}$ protein including G_z[39]. We initially verified the effect of OZITX on the activation of wild-type $G_{i/o/z}$ proteins and G protein chimeras using the G protein nanoBRET assay (Supplementary Fig. 6A). Our data indicate a complete abolishment of signal initiated by wild type $G\alpha_o$, $G\alpha_i$, and $G\alpha_z$, while the inhibition of the Gs-based chimeras was minimal for GsGo and GsGz, and more pronounced but incomplete for GsGi (Supplementary Fig. 6B). We then incorporated OZITX in our assay and tested the activation of D2R, GABABR, ADRA2A, and MOR. Our findings indicate that, overall, OZITX demonstrated a comparable effect to PTX, with no significant enhancement observed in the assay. (Supplementary Fig. 6C).

Multiple conditions can further affect signal detection in G_zESTY

Further conditions can significantly affect assay sensitivity. As previously reported[28], we first confirmed that GloSensor assays produce a greater signal when performed at 28 °C compared to 23 °C or 37 °C (Fig. 3A; Supplementary Fig. 7). Moreover, the presence of ligands in the culturing media can affect GPCR activation because of desensitization processes. We tested this factor by serum starving the cells for 4 hours or changing the cell culture media after transfection to one containing 10% charcoal-stripped FBS or 10% dialyzed FBS (Fig. 3B; Supplementary Fig. 8). Our data showed that serum starvation negatively impacted the signal obtained for three out of four prototypical GPCRs. However, we cannot rule out the possibility that serum starvation might enhance signal detection for other GPCRs, thus we recommend testing this condition for each receptor of interest. Furthermore, many GPCRs have been shown to interact with extracellular matrix components[40] and, therefore, the analysis of their signaling

https://doi.org/10.1038/s41467-025-59850-8

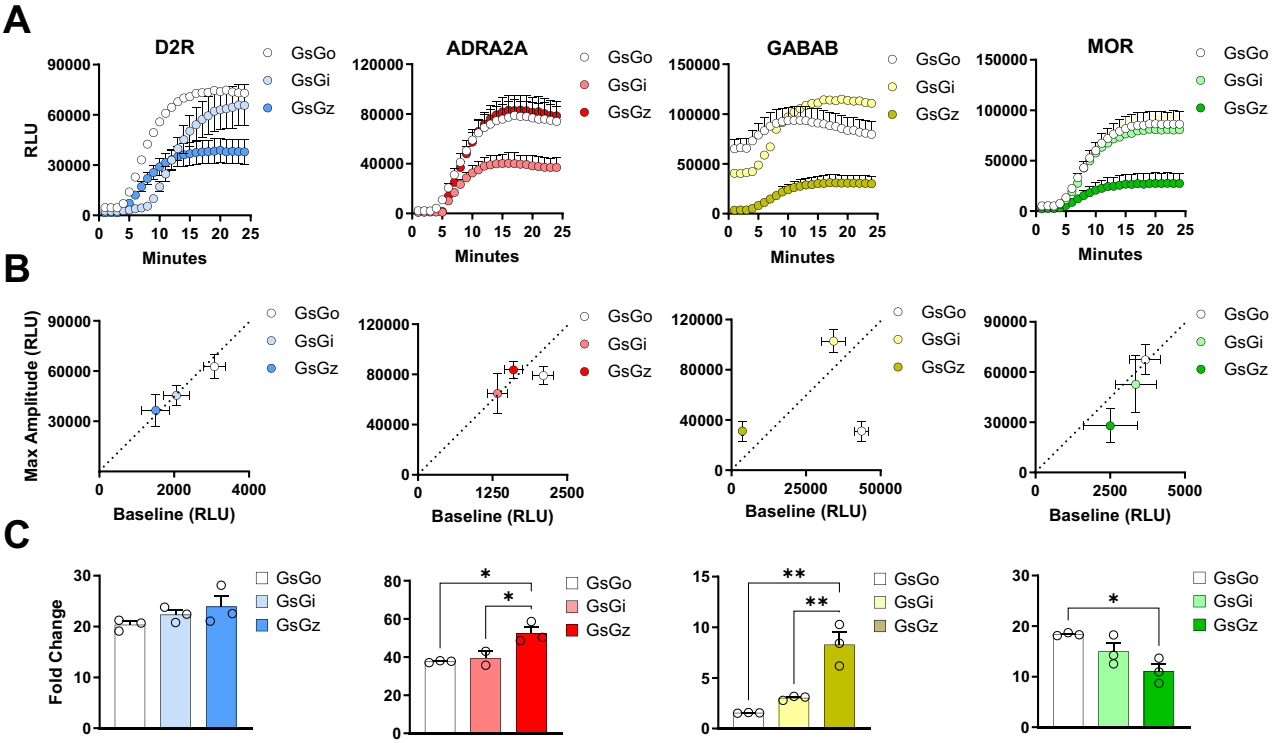

Fig. 1 | Real-time activation of Gs-based chimeras by $G_{i/o/z}$-coupled receptors. **A** Kinetics of cAMP accumulation in response to agonist stimulation of indicated GPCRs using 10 μM dopamine, 10 μM clonidine, 10 μM GABA, and 1 μM DAMGO, respectively. **B** Correlation between maximal amplitude and basal signal for each receptor co-expressed with indicated G protein chimeras. **C** Fold change calculated as the ratio of maximal amplitude over baseline reported in panel (**B**). Data are shown as means ± SEM. $N = 3$ independent replicates (one-way ANOVA with Tukey's multiple comparisons test, $^*p < 0.05$; $^{**}p < 0.01$). In (**C**), $^*p = 0.0155$ ADRA2A GsGo vs GsGz, $^*p = 0.0383$ ADRA2A GsGi vs GsGz, $^*p = 0.0167$ for MOR GsGo vs GsGz, $^{**}p = 0.0011$ for GABAB GsGo vs GsGz, $^{**}p = 0.0039$ for GABAB GsGi vs GsGz, $^*p = 0.0167$ for MOR GsGo vs GsGz.

properties may be different if studied using cells in adhesion or in suspension. We tested the same four GPCRs in these two conditions and we found that, indeed, GABAB receptor shows a significantly higher signal when cells are cultured in poly-D-lysine coated wells (Fig. 3C; Supplementary Fig. 9). Finally, we tested the possible advantage of blocking endogenous phosphodiesterases (PDEs) with IBMX to enhance the accumulation of cAMP (Fig. 3D; Supplementary Fig. 10). As expected, we found that applying IBMX before recording the baseline significantly increased the baseline reading and reduced the overall fold change observed. However, when IBMX was applied at the same time as the agonist, we measured a significant increase in signal (Fig. 3D; Supplementary Fig. 10). By subtracting the signal obtained by applying IBMX with the vehicle from the total luminescence observed, we found that the increased signal was not simply due to the simultaneous activation of adenylyl cyclase and inhibition of PDEs. From here on, we applied the optimized G_zESTY protocol as summarized: plasmids were co-transfected at a molar ratio of 50:47.5:1.8:0.7 (GloSensor:GPCR:GsGz:PTX-S1) in a media containing 10% dialyzed FBS; the assay was run at 28 °C; and 50 μM IBMX was co-applied with agonists.

To quantify the robustness of G_zESTY, we calculated a screening window coefficient (Z factor). This factor reflects both the dynamic range of the assay and its variability, and it is a significant metric of the assay quality. Considering the overall goal of using G_zESTY for GPCR deorphanization where agonists are normally not available, we calculated the Z factor in two different conditions. We first compared cells transfected with D2R or GABAB receptors and treated with the respective agonist vs vehicle (Fig. 3E; Supplementary Fig. 11A). Then, we analyzed the effect of agonist treatments on cells expressing each GPCR vs mock-transfected cells (Fig. 3F; Supplementary Fig. 11B). This condition mimics the conditions for high-throughput screening to identify orphan GPCR ligands. Independent replicates conducted on different days demonstrated that the assay is reproducible, with Z factors calculated at 0.75 and 0.83 for D2R, and 0.78 for both conditions for the GABAB receptor (Fig. 3G; Supplementary Fig. 11C).

Generation of an all-in-one plasmid for G_zESTY cell delivery

Like most cell-based systems used to detect GPCR signaling, G_zESTY is a multicomponent assay (Fig. 4A). As a result, functional measurements require efficient co-delivery of multiple plasmids in each cell. This issue is normally overcome by averaging the signal of a large number of cells assuming that a significant fraction will express all the components. We recently generated a facile system to produce large plasmids encoding multiple proteins under the control of individual promoters. This approach guarantees that each transfected cell will express all of the necessary components, thereby increasing the assay's sensitivity and simplifying transfection protocols. To select promoters to drive the expression of each component recapitulating our previously defined ratios, we performed a promoter efficiency assay (Fig. 4B). Based on these results, we selected a minimal CMV promoter to express the GloSensor and GPCRs, and a UbC promoter for the expression of PTX-S1 and GsGz. We subcloned each component accordingly and generated a set of all-in-one plasmids (Fig. 4C). We then tested these newly generated tools in cells transiently transfected with each of our four prototypical $G_{i/o/z}$-coupled receptors that we stimulated with selective agonists. We found that the 4-in-one plasmids performance was comparable to the co-transfection of multiple plasmids, but greatly simplified transfection protocols and reproducibility (Fig. 4D). Interestingly, the receptor expression from the 4-in-one plasmid was significantly lower compared to transfecting

https://doi.org/10.1038/s41467-025-59850-8

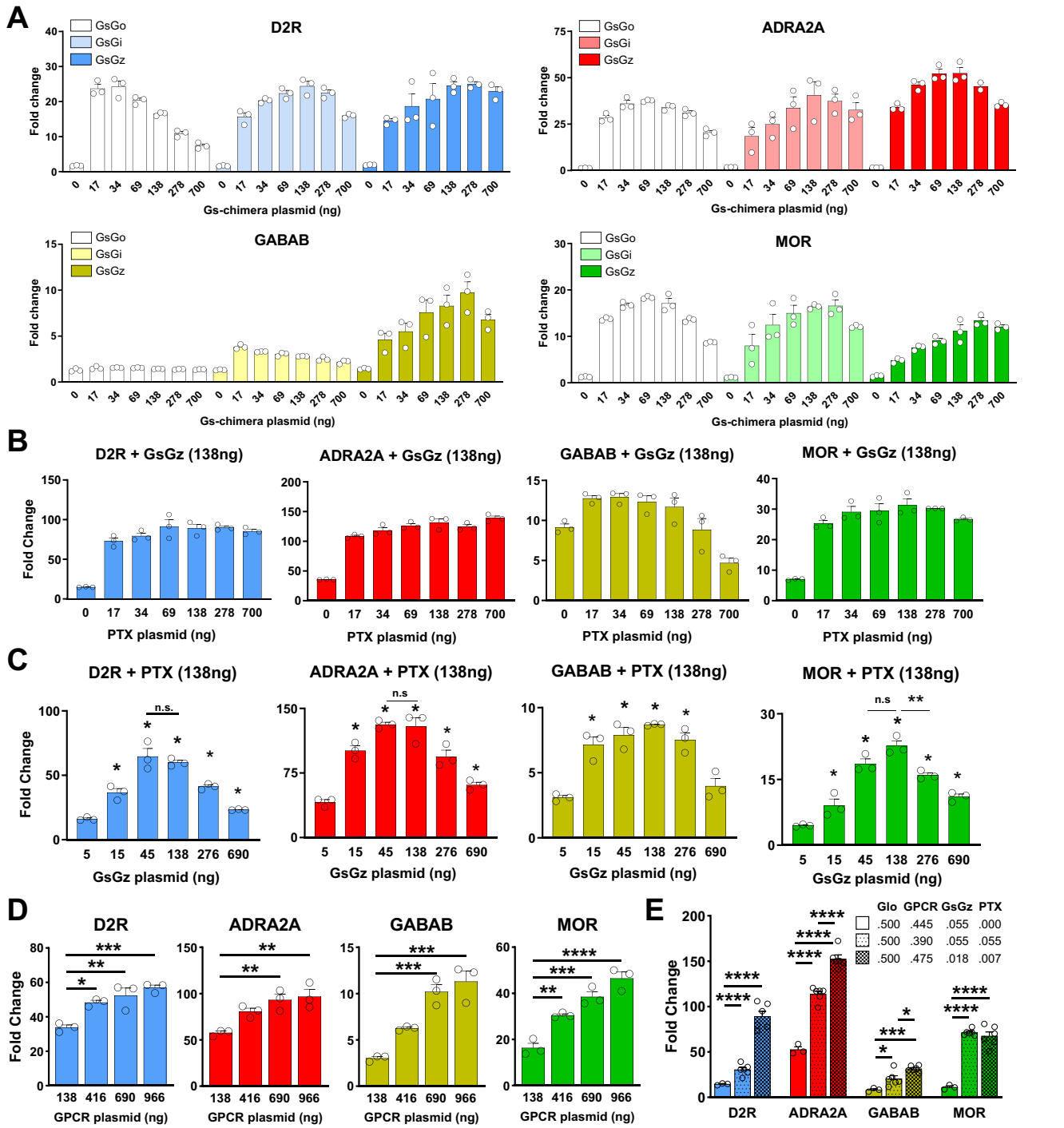

Fig. 2 | Optimization of transfection ratios between G_zESTY components. **A** Activation of indicated GPCRs with increasing amount of transfected Gs-based chimeras. $N = 3$ independent experiments. **B** GPCR activation with the introduction of increasing concentrations of PTX-S1 subunit to eliminate the inhibition of adenylyl cyclase by endogenous $G_{i/o}$ proteins. N=3 independent experiments. **C** GPCR activation in the presence of increasing amount of transfected GsGz plasmid. $N = 3$ independent experiments. **D** Signal fold change with titration of each transfected receptor. $N = 3$. **E** Fold-change comparison between standard transfection ratio and optimized ratio 50:47.5:1.8:0.7 (GloSensor:GPCR:GsGz:PTX). The data shown represent the average of 3–6 independent experiments ($N = 3$–6) (one-way ANOVA with Dunnett's multiple comparisons test, $^{*}p < 0.05$; $^{**}p < 0.01$; $^{***}p < 0.001$; $^{****}p < 0.0001$). Data are shown as means ± SEM.

individual plasmids; however, this does not impact assay performance (Supplementary Fig. 12).

Next, we expanded the analysis of G_zESTY capabilities to a larger array of 24 $G_{i/o/z}$-coupled GPCRs paired with the 3-in-one construct. We confirmed the suitability of the assay to study the pharmacology of 23 out of 24 $G_{i/o/z}$-coupled receptors (Fig. 5A, C). At the same time, we confirmed that in our setup we can still detect the activation of 5 G_s-coupled receptors (Fig. 5A). The majority of GPCRs exhibit a primary, preferential coupling to a single G protein family, such as G_s, $G_{i/o/z}$, G_q, or $G_{12/13}$. However, it is uncommon for a GPCR to only activate one G protein family, as secondary coupling to additional G proteins is typical[41,42]. To test whether G_zESTY could detect the activation of

https://doi.org/10.1038/s41467-025-59850-8

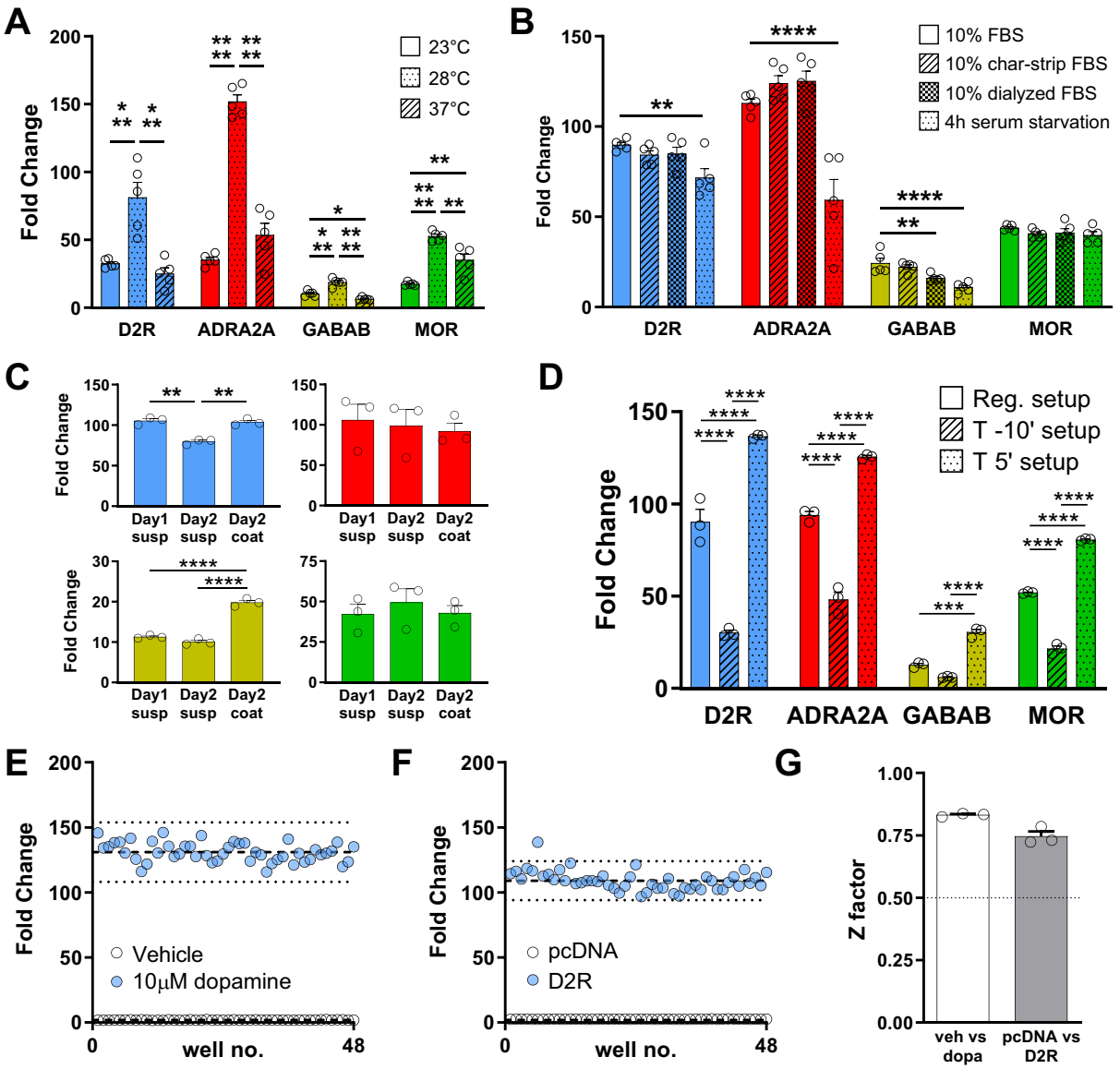

Fig. 3 | G_zESTY protocol optimization and Z factor calculation. A Assay temperature influences assay sensitivity. Assays performed at 28 °C give a significantly higher signal. $N = 5$ independent experiments. **B** FBS removal (4 h serum starvation), use of charcoal-stripped FBS, or use of dialyzed FBS did not improve the assay signal. $N = 5$ independent experiments. **C** Assays performed with cells in adhesion show a signal improvement for GABAB receptor but not for D2R, ADRA2A, and MOR. $N = 3$ independent experiments. **D** Co-treatment with 50 μM IBMX (T 5′ setup) significantly increases the signal with each of the four GPCRs. Data shown represent the average of 3 independent experiments ($N = 3$). The effect of IBMX alone was subtracted from each experimental condition. One-way ANOVA with Dunnett's multiple comparisons test, $^{*}p < 0.05$; $^{**}p < 0.01$; $^{***}p < 0.001$; $^{****}p < 0.0001$. Data are shown as means ± SEM. **E** Cells transiently transfected with D2R were treated with either 10 μM dopamine or vehicle. Dashed lines represent the means of the fold change. Dotted lines display three standard deviations from the mean of each data set. **F** Cells transfected with indicated plasmids were treated with 10 μM dopamine. Dashed lines represent the means of the fold change for cells expressing D2R or cells not expressing exogenous GPCRs (pcDNA, control). **G** Z factor calculation. Dotted lines indicate the threshold for robust assays. Data shown in panels (**E** and **F**) are representative of three independent experiments quantified in panel (**G**) as means ± SEM.

GPCRs that do not exhibit a primary coupling to G_s or $G_{i/o/z}$, we analyzed three additional GPCRs: 5-HT2AR, M3R, and GPR55 in response to the application of selective agonists (Supplementary Fig. 13A). The response detected by G_zESTY suggests that even with minimal secondary coupling to $G_{i/o/z}$, both 5-HT2AR and M3R showed a robust signal, while GPR55 showed no detectable signal (Supplementary Fig. 13B). Overall, this data demonstrated that G_zESTY is a powerful tool for GPCR deorphanization as it sensitively detects activation of both primarily and secondarily coupled $G_{i/o/z}$- and G_s-coupled GPCRs, potentially enabling the study of 86% of the GPCRome and, by similarity, most of the orphan GPCRs (Fig. 5B).

We next investigated if G_zESTY was suitable to detect partial agonism. Using MOR as a model, we obtained concentration-response curves after stimulation with the endogenous ligand β-endorphin (pEC50 = 5.45, $E_{max} = 62.91$), with the full agonist DAMGO (pEC50 = 7.17; $E_{max} = 59.53$), and with the partial agonist morphine (pEC50 = 7.21, $E_{max} = 38.85$) that showed 65% of the maximal amplitude measured with DAMGO (Fig. 6A). We also demonstrated that G_zESTY can be used to study the activation of endogenously expressed receptors. To this goal, concentration-response curves were obtained from cells transfected with the 3-in-one construct, which does not express any exogenous GPCR, and treated with selective peptidic

https://doi.org/10.1038/s41467-025-59850-8

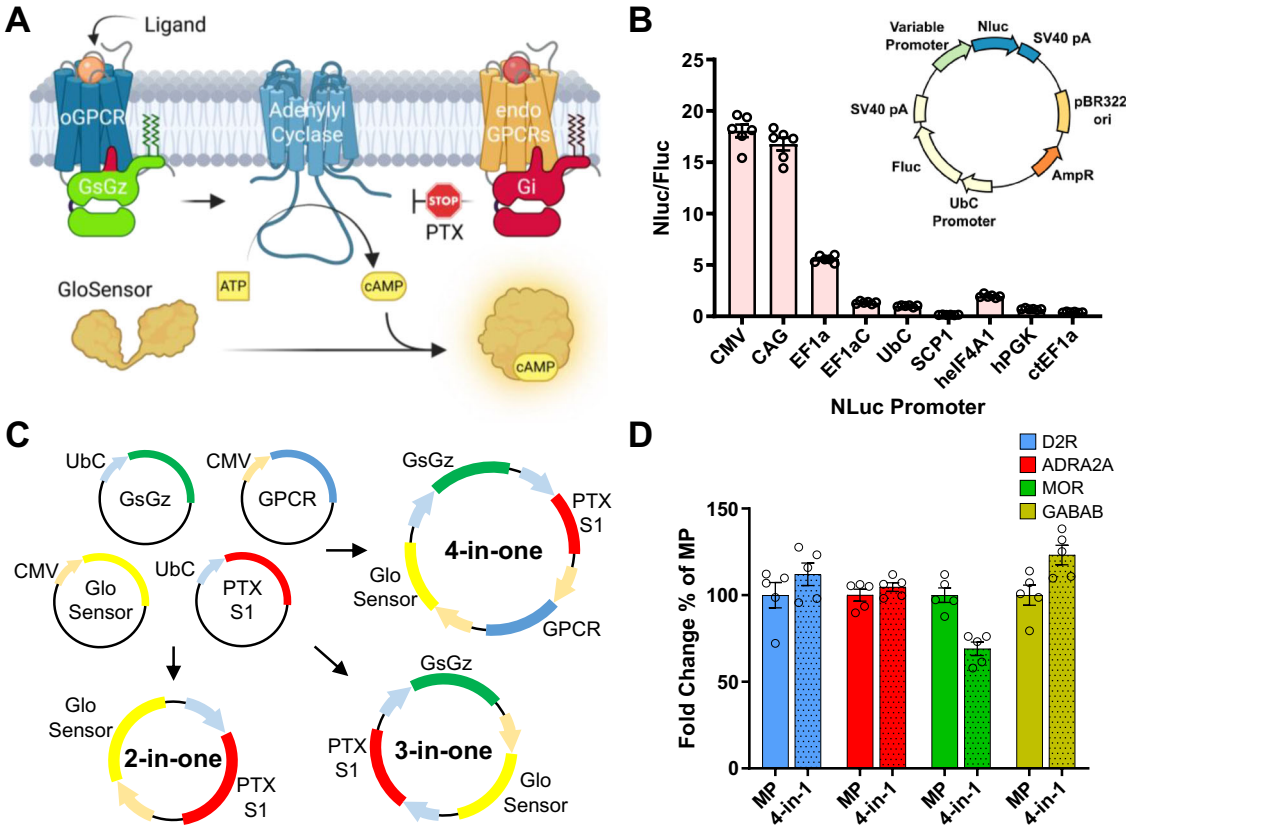

Fig. 4 | All-in-one G_zESTY plasmids. A Schematics of G_zESTY and each of its components (created in BioRender. Orlandi, C. (2025) https://BioRender.com/hs1vfma). **B** Promoter efficiency estimation calculated as Nluc luminescence normalized over firefly luminescence signal in HEK293 cells transfected with a plasmid encoding nanoluc under the control of each of the indicated promoters and firefly under the control of UbC promoter. Data are shown as means ± SEM; $N = 6$ independent transfections. **C** Maps of the all-in-one plasmids generated. **D** Assay comparison in cells transiently transfected with four single plasmids or with each of the 4-in-one plasmids encoding each indicated GPCR. MP multiple plasmids. Data are shown as means ± SEM; $N = 5$ independent transfections.

agonists activating endogenously expressed protease-activated receptor (PAR) PAR1 ($pEC50 = 4.56$, $E_{max} = 73.87$) or PAR2 ($pEC50 = 4.97$, $E_{max} = 103.70$). Cells transfected with the 2-in-one construct (no GsGz chimera) served as negative control (Fig. 6B). We further applied G_zESTY to screen the activation of our four prototypical GPCRs by 84 compounds included in the SCREEN-WELL Orphan ligand library. This library is a rich source of ligands for receptor deorphanization as it includes endogenous compounds with putative or potential biological activity, whose cellular targets are currently unknown (Fig. 6C). As positive controls, we included the selective agonist for each of the receptors studied. This analysis revealed several hit compounds activating ADRA2A and D2R. Using the orthogonal G protein nanoBRET assay, we validated some of these hits and obtained concentration-response curves (Fig. 6D). We found that salsolinol-1-carboxylic acid acts as a D2R agonist ($pEC_{50} = 5.84$; $E_{max} = 85.07$) and we compared it to dopamine ($pEC_{50} = 8.27$; $E_{max} = 89.61$). Similarly, we discovered endogenous partial agonists acting on ADRA2A including tryptamine ($pEC_{50} = 5.86$; $E_{max} = 46.65$), 3-hydroxyphenethylamine ($pEC_{50} = 6.11$; $E_{max} = 48.53$), octopamine ($pEC_{50} = 6.32$; $E_{max} = 69.74$), and we compared them with norepinephrine ($pEC_{50} = 8.31$; $E_{max} = 92.86$). This set of data provides further evidence of the applicability of G_zESTY for high throughput screening and identification of novel compounds activating GPCRs.

G_zESTY application to GPCR deorphanization

To assess the suitability of G_zESTY in projects aiming at the identification of endogenous ligands for orphan GPCRs, we treated cells co-transfected with the 3-in-one plasmid and individual GPCRs with a raw source of endogenous ligands. Historically, similar strategies were successfully used to isolate anandamide from pig brain, identifying it as an endogenous ligand for cannabinoid receptors[43]; these methods also facilitated the identification of ghrelin from rat stomach extract[44], and helped pair other GPCRs with their endogenous ligands[45–48]. Here, we prepared several mouse brain extracts following the pipeline outlined in Fig. 7A, which we applied to G_zESTY-transfected cells to measure cAMP accumulation over time. In these experiments, we compared the effects of applying whole brain homogenates with those of two fractions obtained after centrifugation (supernatant and resuspended pellet), both with and without microwaving the brain. Control cells transfected with the 3-in-one plasmid and therefore expressing GloSensor, GsGz, and PTX, but not exogenous GPCRs, showed significant induction of cAMP levels likely due to the activation of endogenous receptors. Notably, we observed differences in receptor activation, suggesting that simple procedures like centrifugation and microwaving can aid in isolating specific endogenous GPCR ligands (Fig. 7B). Interestingly, microwaving significantly enhanced the activation of endogenous GPCRs expressed in HEK293 cells, as well as transfected receptors. While ADRA2A signaling was detected under all conditions, MOR activation was more pronounced with supernatant fractions and exhibited a higher signal when the brain was microwaved, in agreement with previous reports showing how microwave irradiation could preserve neuropeptides from degradation[49] (Fig. 7B). As a proof of specificity, we applied brain extract (no-mw-supernatant extraction protocol) in the presence of specific GPCR antagonists (Fig. 7C). This experiment demonstrated that the observed signal increase, resulting from applying brain extract to cells transfected with

https://doi.org/10.1038/s41467-025-59850-8

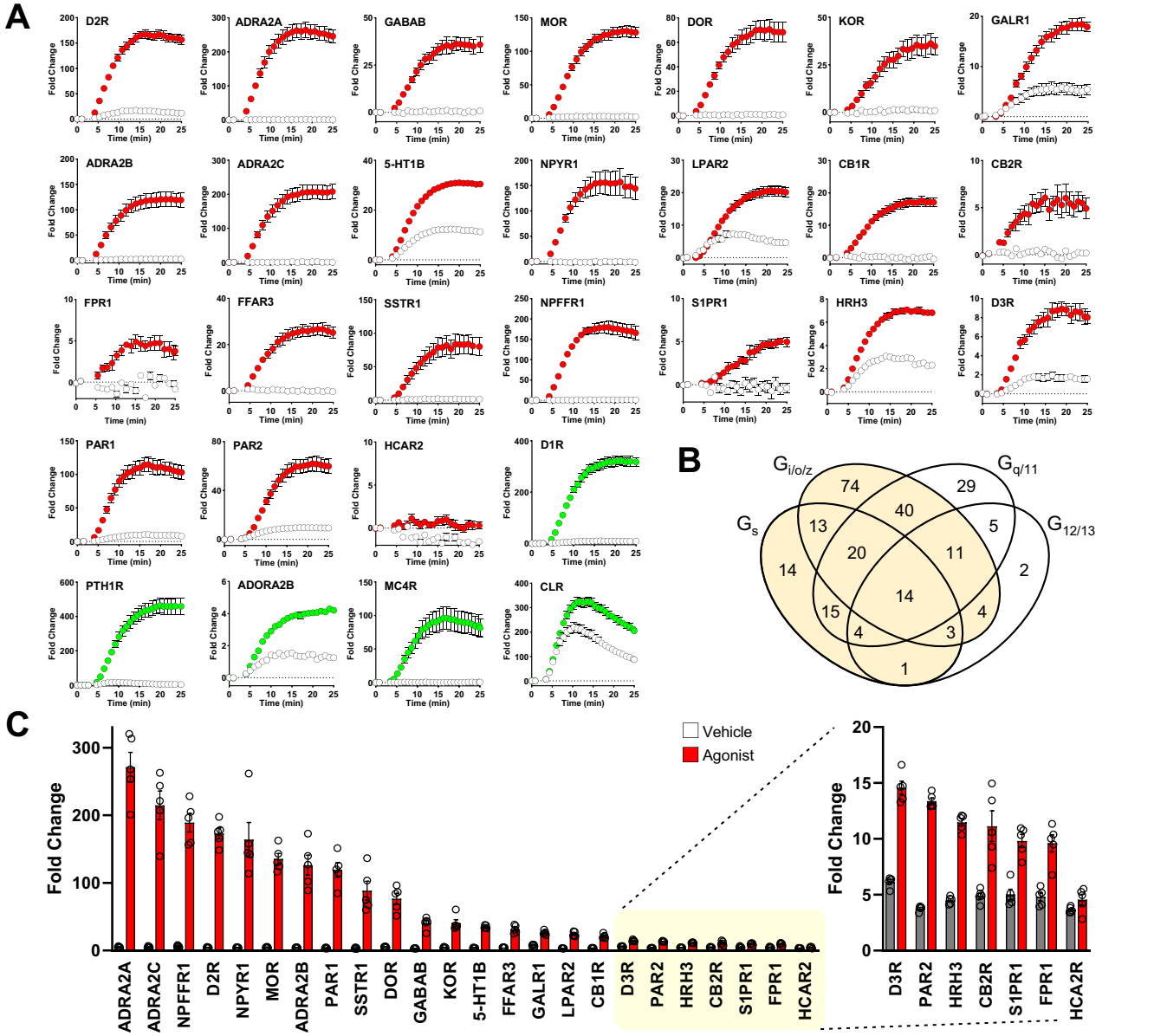

Fig. 5 | G$_z$ESTY applied to a battery of ligand-activated GPCRs. A Real-time analysis of ligand-mediated activation of a battery of $G_{i/o/z}$-PCRs (red) and G_s-PCR (green) in cells co-transfected with indicated receptors and the 3-in-one G$_z$ESTY plasmid in the presence of 50 μM IBMX. Cells transfected only with the 3-in-one plasmid served as control (white). The following agonists were applied at 4 min: 10 μM dopamine (D2R, D1R), 100 μM clonidine (ADRA2A, ADRA2B, ADRA2C), 10 μM GABA (GABABR), 10 μM DAMGO (MOR), 1 μM SNC-80 (DOR), 10 μM salvinorin A (KOR), 10 μM human galanin (1–30) (GAL1R), 100 μM serotonin (5-HT1B), 10 μM human neuropeptide Y (13–36) (NPYR1), 10 μM lysophosphatidic acid (LPAR2), 10 μM 2-arachidonoyl glycerol (CB1R, CB2R), 10 μM N-formyl-met-leu-phe (FPR1), 1 mM isobutyric acid (FFAR3), 10 μM somatostatin 14 (SSTR1), 10 μM neuropeptide FF (NPFFR1), 10 μM SEW2871 (S1PR1), 10 μM histamine (HRH3), 10 μM quinpirole (D3R), 10 μM TFLLR (PAR1), 10 μM SLIGKV (PAR2), 10 μM MK-6892 (HCA2R), 1 μM teriparatide PTH (PTH1R), 10 μM AB-MECA (ADORA2B), 10 μM NDP-α-MSH (MC4R), and 10 μM CGRP (CLR). Data are shown as means ± SEM; $N = 5$ independent transfections. **B** GPCRs that couple to G_s and/or $G_{i/o/z}$ and can potentially be detected by GZESTY are highlighted and include 213 out of 249 total ligand-activated GPCRs (86%) (adapted from GPRCdb.org). **C** Quantification of agonist-induced activity for 24 $G_{i/o/z}$-coupled GPCRs. On the right, the response to agonist of the last seven GPCRs is also reported with a different scale. Data are shown as means ± SEM of the fold change obtained; $N = 5$ independent transfections.

specific GPCRs, is dependent on the GPCR itself rather than on other potential cellular mechanisms. As an additional control for specificity, we investigated D2R activation in response to the application of no-mw-supernatant extracts from the striatum and cerebellum (Fig. 7D). Our ELISA confirmed striatal enrichment in dopamine (1216.00 ± 991.18 nM) compared to cerebellum samples (8.96 ± 7.49 nM). As expected, striatum extract induced significantly greater D2R activation compared to the cerebellum extract. We also conducted a series of assessments to further investigate the composition of the applied brain extracts. We used ELISA to measure dopamine and norepinephrine levels in the six different extract preparations. Additionally, we quantified levels of proteins, unsaturated fatty acids, and we assessed absorbance ratios (260/230 and 280/230) to estimate nucleic acid content in each fraction (Table 1).

In parallel, we applied the same strategy to explore the possible activation of a battery of orphan GPCRs from brain extracts. Intriguingly, we detected a consistent activation of orphan receptors GPR37 and GPR176 suggesting a significant presence of their endogenous

https://doi.org/10.1038/s41467-025-59850-8

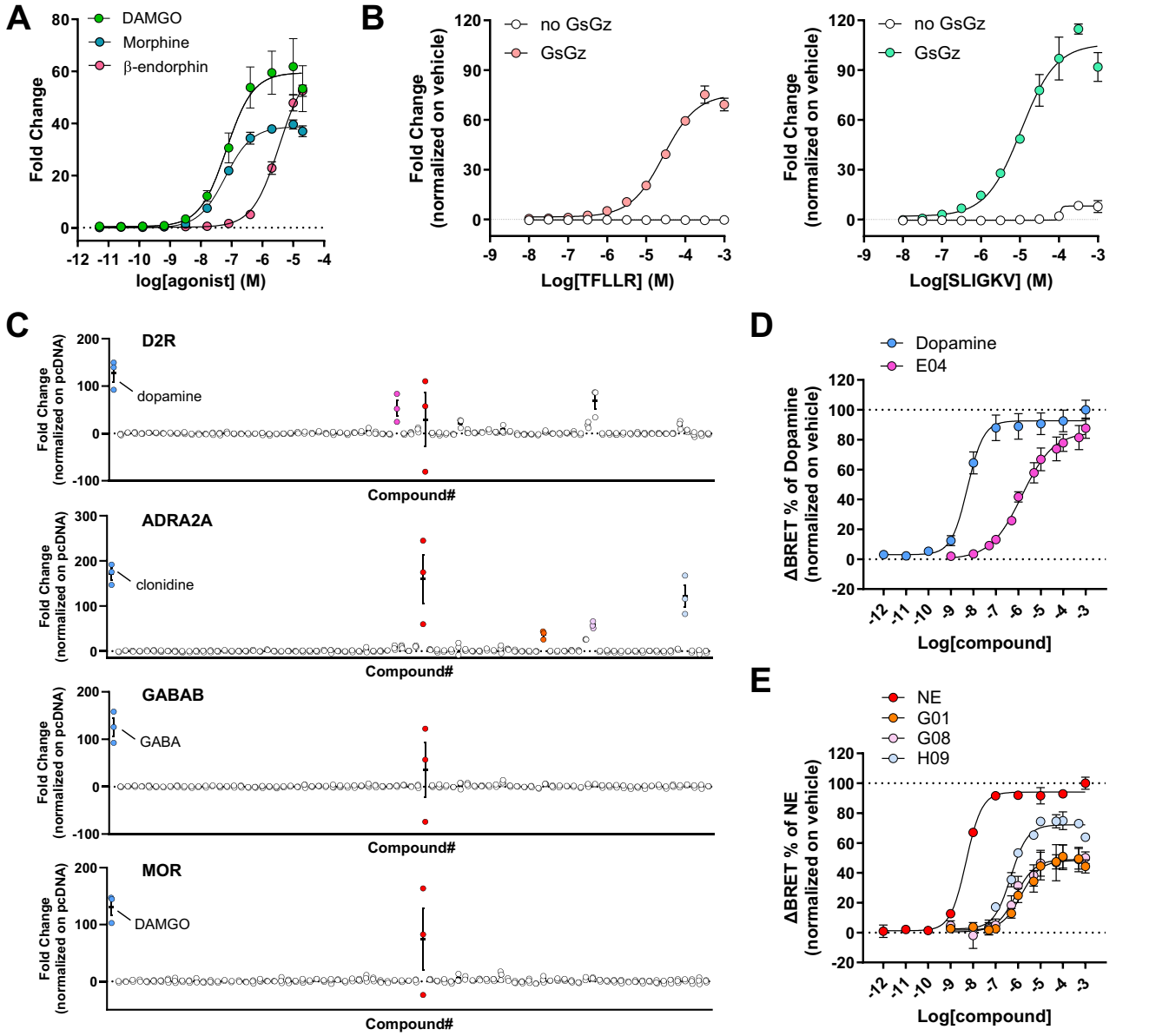

Fig. 6 | G_zESTY applications. A Concentration-response curves obtained for MOR stimulated with DAMGO, morphine, or β-endorphin. Data are shown as means ± SEM; $N = 3$ independent transfections. **B** Concentration-response curves of endogenously expressed PAR1 activated with a selective agonist peptide TFLLR (left) or PAR2 activated with selective agonist peptide SLIGKV (right) in cells transfected only with the 3-in-one plasmid. Control cells were transfected with a 2-in-one plasmid not expressing GsGz chimera. Data are shown as means ± SEM; $N = 3$ independent transfections. **C** Results obtained applying G_zESTY to screen the small library of orphan ligands, 84 compounds with putative or potential biological activity, whose cellular targets are currently unknown (Enzo Life Sciences SCREEN-WELL orphan ligand library). In blue are positive control agonists for each receptor; in red is a common hit likely activating an endogenously expressed GPCR (dihydroxynorephedrine). Data are shown as means ± SEM; $N = 3$ independent transfections. **D** Concentration-response curves obtained using G protein nanoBRET assay to validate positive hits activating D2R with compound E04 (salsolinol-1-carboxylic acid) or dopamine. Data are shown as means ± SEM; $N = 3$ independent transfections. **E** Concentration-responses for ADRA2A activated in response to the application of compounds G01 (tryptamine), G08 (3-hydroxyphenethylamine), H09 (octopamine), or norepinephrine (NE). Data are shown as means ± SEM; $N = 3$ independent transfections.

ligands in the mouse brain (Fig. 7B). While GPR37 activation required the microwave step but was independent from further centrifugation steps, signal from GPR176 was only detected in the supernatant of microwaved samples (Supplementary Fig. 14). Both these orphan GPCRs are expressed in the brain, and they are reported to couple to heterotrimeric G proteins of the $G_{i/o/z}$ family, but their endogenous ligands have not been identified or agreed upon[50–52]. Using the same strategy, we tested the presence of GPCR ligands in bovine pituitary extracts. We reasoned that many GPCRs are activated by hormones released by glands, and we used the follicle-stimulating hormone (FSH) receptor as a positive control, as its endogenous ligand is secreted by the pituitary gland. We found that pituitary extract can indeed activate FSHR, but none of the orphan GPCRs we tested were activated (Fig. 7E).

Discussion

Orphan GPCRs, by definition, have unknown or poorly understood ligands and signaling mechanisms. Without a known ligand or baseline receptor activity, designing assays to measure their activation or inhibition becomes a complex task. A major obstacle in identifying endogenous ligands for orphan GPCRs is the absence of sensitive

https://doi.org/10.1038/s41467-025-59850-8

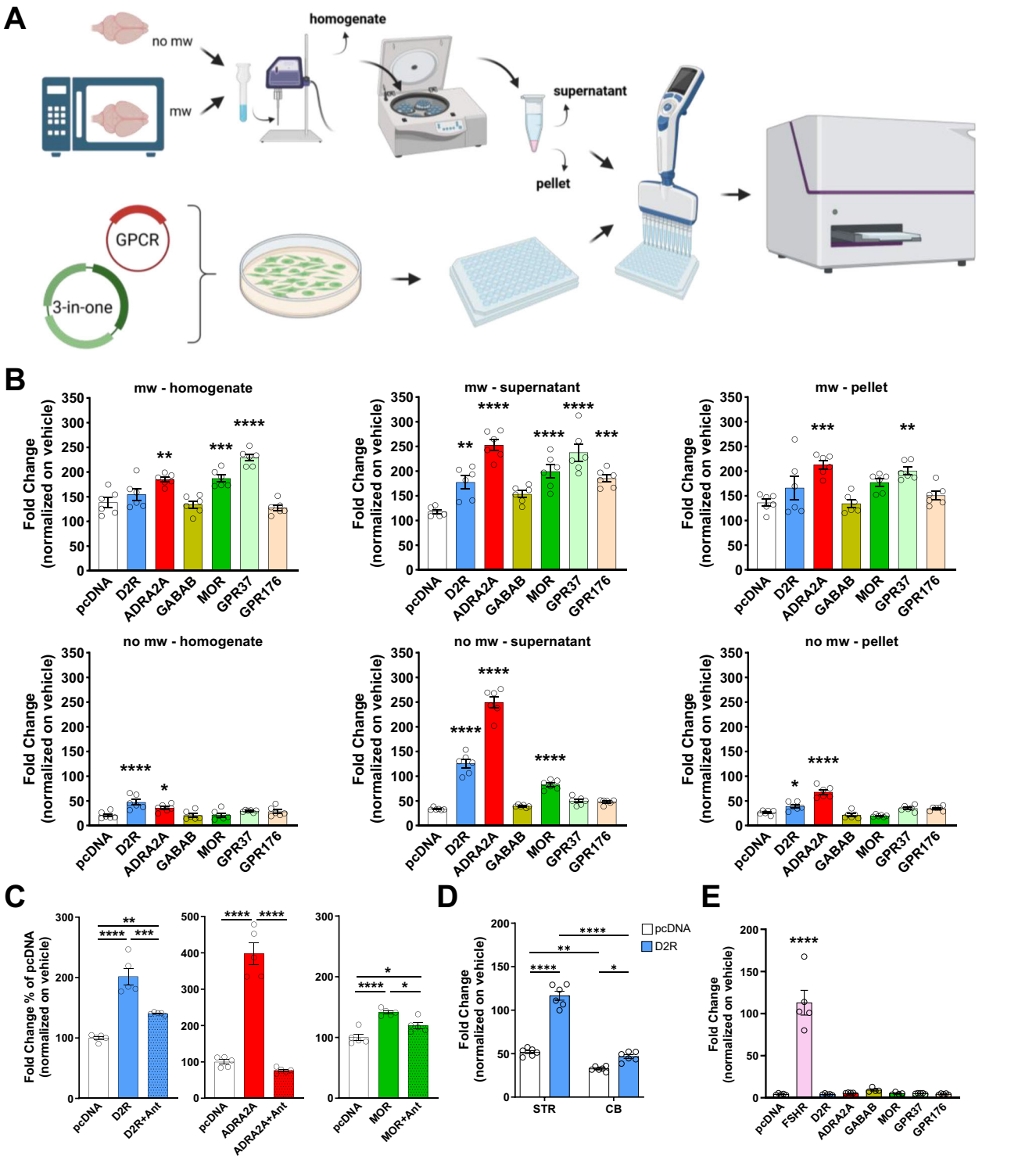

assays capable of detecting low concentrations of these ligands in biological samples. This challenge is especially pronounced for orphan GPCRs that couple to heterotrimeric G proteins of the $G_{i/o/z}$ family, which, according to the G protein database (GPCRdb.org), represent 72% of deorphanized GPCRs, with 30% being uniquely coupled to $G_{i/o/z}$ proteins[41,42]. To address this problem, we designed G_zESTY, an optimized cell-based assay that enables robust detection of GPCR activation in response to both purified ligands and mixed sources of molecules, including those containing diluted ligands. The standard approach for measuring $G_{i/o/z}$-coupled receptor activation of wild-type G proteins is indirect, relying on a comparison between cells treated with vehicle and those pre-incubated with an agonist before forskolin-mediated stimulation of adenylyl cyclase, assessing the reduction in cAMP accumulation. In contrast, G_zESTY detects the activation of $G_{i/o/z}$-coupled receptors as a direct response to agonist application. To compare G_zESTY with a traditional cAMP inhibition assay, we obtained concentration-response curves for D2R activated by the full agonist quinpirole (Supplementary Fig. 15A). Both G_zESTY (Supplementary Fig. 15B) and the cAMP inhibition assay (Supplementary Fig. 15C) demonstrated significant signal detection at 1 nM quinpirole. However,

Fig. 7 | Analysis of GPCR activation by tissue extract application using G_zESTY. **A** Schematics of the protocol applied to prepare six different brain extracts: no-mw-homogenate, no-mw-supernatant, no-mw-pellet, mw-homogenate, mw-supernatant, and mw-pellet. Brain homogenates were sonicated and centrifuged to obtain a supernatant fraction, and a pellet that was resuspended in PBS and further sonicated. Each fraction was then applied to cells transfected with G_zESTY and distributed in 96-well plates. cAMP levels were measured before and after brain extract application for a total of 25 min (created in BioRender. Orlandi, C. (2025) https://BioRender.com/f88k131). **B** The six different brain extract preparations induce different level of activation of D2R, ADRA2A, MOR, GPR37 and GPR176. One-way ANOVA with Dunnett's multiple comparisons test, $^{*}p < 0.05$; $^{**}p < 0.01$; $^{***}p < 0.001$; $^{****}p < 0.0001$. Data are shown as means ± SEM; $N = 6$. **C** Co-application of 10 μM of selective GPCR antagonists occlude the brain-induced activation of D2R, ADRA2A, and MOR. Antagonists applied were: L-741626 (D2R), RS-79948 (ADRA2A), and naloxone (MOR). One-way ANOVA with Tukey's multiple comparisons test, $^{*}p < 0.05$; $^{**}p < 0.01$; $^{***}p < 0.001$; $^{****}p < 0.0001$. Data are shown as means ± SEM; $N = 5$. **D** Quantification of D2R response to application of no-mw extracts obtained from mouse striatum (STR) or cerebellum (CB). Cells transfected with pcDNA served as negative control. Two-way ANOVA with Tukey's multiple comparisons test, $^{*}p < 0.05$; $^{**}p < 0.01$; $^{****}p < 0.0001$. Data are shown as means ± SEM; $N = 6$. **E** Quantification of indicated GPCR activation in response to application of bovine pituitary extract. FSH receptor served as a positive control and pcDNA as negative control. One-way ANOVA with Dunnett's multiple comparisons test, $^{****}p < 0.0001$. Data are shown as means ± SEM; $N = 4$–5; mw microwaved, no mw not microwaved.

Table 1 | Analytical measurements of brain extract content

	Microwaved brain extracts			Non-microwaved brain extracts		
	Homogenate	Supernatant	Pellet	Homogenate	Supernatant	Pellet
Nucleic acids (μg/μL)	3.15 ± 0.54	0.38 ± 0.03	3.12 ± 0.49	3.48 ± 0.55	0.48 ± 0.05	3.30 ± 0.33
260/280	1.14 ± 0.01	2.21 ± 0.06	1.09 ± 0.03	1.12 ± 0.01	1.56 ± 0.02	1.09 ± 0.02
260/230	0.67 ± 0.02	1.62 ± 0.05	0.60 ± 0.01	0.62 ± 0.01	0.58 ± 0.01	0.64 ± 0.04
Proteins (μg/μL)	18.70 ± 4.38	0.28 ± 0.14	16.53 ± 1.64	11.9 ± 7.01	1.73 ± 0.15	13.36 ± 1.56
Unsaturated FAs (mg/brain)	95.83 ± 22.03	2.98 ± 1.91	72.05 ± 39.84	43.51 ± 7.44	5.54 ± 0.16	43.98 ± 5.21
NE (nM)	38.9 ± 5.26	35.6 ± 1.45	11.9 ± 3.81	45.73 ± 2.95	39.5 ± 4.30	32.58 ± 2.13
DA (nM)	412.2 ± 246.5	289.5 ± 40.4	76.41 ± 35.4	337.1 ± 79.4	133.6 ± 24.9	191.6 ± 62.1

Values expressed as the mean of 3 experiments ± SD.

we believe that G_zESTY offers several advantages: **1**. By measuring an increase instead of a decrease in luminescence, G_zESTY enables a greater dynamic range; **2**. G_zESTY does not require pre-treatments with forskolin or isoproterenol, consequently, experimental protocols are simplified. In traditional $G_{i/o/z}$-mediated cAMP inhibition assays, a range of forskolin concentrations are used ranging from 0.5 μM to 100 μM[53–61]. Sometimes agonists activating endogenously expressed G_s-coupled receptors (i.e. isoproterenol) are utilized instead of forskolin[61–63]. Moreover, a range of ligand pre-incubation ranging from 0 to 15 min further increases the experimental variability[53–61]. None of these parameters are part of the G_zESTY protocol; **3**. Since transfection efficiency is rarely 100% and only a subset of cells successfully incorporates multiple plasmids, stimulating endogenously expressed adenylyl cyclase with forskolin may lead to cAMP accumulation in cells that do not express the GPCR of interest. This could reduce the sensitivity of the cAMP inhibition assay. G_zESTY addresses this problem by eliminating the need to stimulate adenylyl cyclase with forskolin or isoproterenol, and, with our all-in-one format, ensuring that all transfected cells express each assay component, resulting in more consistent transfection across the cell population; **4**. We observed that while the cAMP inhibition assay can effectively detect MOR activation by three different ligands, it cannot discriminate between partial agonists and full agonists as effectively as G_zESTY (Supplementary Fig. 15D). This is likely due to a ceiling effect: once a certain level of inhibition is reached, it becomes increasingly difficult to detect additional inhibition quantitatively. In contrast, with G_zESTY, we measure cAMP accumulation, a process that is more difficult to saturate, thereby minimizing the likelihood of reaching a ceiling effect; finally, **5**. considering G_zESTY's capability to detect the presence of endogenous ligands in complex sources such as brain extracts, we explored the performance of the traditional cAMP inhibition assay in the same task (Supplementary Fig. 15E). This assay cannot be performed according to the standard protocol where the application of an agonist is compared to the application of a vehicle to calculate the inhibition in cAMP production. Instead, the same population of cells was treated with microwaved mouse brain extract (serving as the "agonist") and 10 μM forskolin, while, in the control experiment, 10 μM of selective antagonists were also co-applied. Overall. our data indicates that a traditional cAMP inhibition assay is less sensitive than G_zESTY for this task (Supplementary Fig. 15F).

Our work identified optimal assay conditions that apply to each GPCR tested, such as the temperature of the assay, ratio of assay components, and presence of IBMX, while other parameters appear to affect the readout in a GPCR-specific manner. For example, we observed a negative effect of serum starvation on the signal obtained for three out of four prototypical receptors, however, the presence of ligands in the culture media has been shown to induce receptor desensitization and internalization halting the access of extracellular ligands to the receptor itself[64–66]. Therefore, we cannot exclude the possibility that testing certain GPCRs may benefit from using reduced serum content or dialyzed serum. This aspect will require specific assessment for individual receptors. Using IBMX has the advantage of enhancing the detected signal, thereby improving the assay's sensitivity. Additionally, it helps eliminate false positives in high-throughput screens caused by the presence of phosphodiesterase inhibitors in many compound libraries. By applying innovative cloning techniques, we generated large plasmids that encode multiple proteins under the control of unique promoters. These all-in-one plasmids have the advantage of expressing each component at precisely defined and optimized ratios. Moreover, their use greatly simplifies transfection protocols for large-scale screening efforts. Using all-in-one plasmids, we showed that G_zESTY is suitable to detect the activation of endogenously expressed receptors. Delivery of the 3-in-one plasmid to relevant cell types can be combined with agonist treatment to perform pharmacological studies of receptors of interest in a physiologically relevant context. Our initial optimization steps for G_zESTY were performed using four prototypical GPCRs (D2R, ADRA2A, GABAB, and MOR). The optimized protocol was later applied to an array of 24 $G_{i/o/z}$-coupled GPCRs. The results showed that the great majority exhibited over a 20-fold change in signal compared to baseline, suggesting ideal

signal-to-noise properties for the assay. We also observed smaller signal amplitude for a few receptors. This lower sensitivity may depend on several factors including the presence of endogenous agonists in the culture media that can lead to receptor desensitization or the requirement of performing the assay with cells in adhesion. Transfected receptors may also not be properly expressed, targeted to the plasma membrane, or require accessory proteins to generate functional receptor complexes. Therefore, when working with a specific receptor it is recommended to test multiple assay conditions in the cell type of choice to achieve an optimal assay sensitivity.

Screening efforts to identify orphan GPCR agonists will be markedly enhanced by utilizing G_zESTY. Analysis of the constitutive activity of orphan GPCRs provides valuable information regarding their G protein coupling profile[35,67,68]. Recent studies have shown that, similar to ligand-activated GPCRs, the majority of orphan GPCRs couple to heterotrimeric G proteins of the $G_{i/o/z}$ family. This makes them suitable candidates for analysis using G_zESTY. Furthermore, given the limited understanding of the G protein coupling profile for many orphan GPCRs, a key benefit of G_zESTY is its ability to detect the activation of approximately 86% of GPCRs. This estimate is based on coupling data regarding the number of GPCRs that show a primary or secondary coupling to G_s and/or $G_{i/o/z}$ proteins (Fig. 5B and Supplementary Fig. 13). A minor caveat in the use of G protein chimeras is that their activation kinetics by $G_{i/o/z}$-coupled receptors do not always mirror that of native G proteins. This discrepancy likely depends on regions of the G protein outside of the C-terminus that could affect coupling, but as shown here, do not impact the ability of G_zESTY to effectively detect GPCR activation. Numerous orthogonal assays are available to GPCR pharmacologists to further define the kinetic properties of receptor-dependent G protein activation[69–72]. By screening a small library of compounds with known biological activity but unidentified molecular targets, we identified several that act as agonists or partial agonists of the human D2R and ADRA2A receptors. The endogenous levels of these ligands in the mammalian brain, their production and release mechanisms, and their interactions with established neurotransmitter systems will require further investigation. Although indications of agonistic activity at the tested GPCRs for some of these ligands have been previously reported[73,74], this dataset strengthens the evidence for the effectiveness of G_zESTY in high throughput screening, demonstrating its potential for discovering novel ligands for oGPCRs.

The isolation of orphan GPCR endogenous ligands relies significantly on the availability of methods that can accurately detect their presence in raw unfractionated extracts. In this study, we utilized G_zESTY to identify the existence of endogenous ligands for orphan GPCRs in mouse brain extracts. Our approach consistently detected known neurotransmitters capable of activating adrenergic, dopaminergic, and opioid receptors, thereby validating the method. Notably, we also identified the presence of ligands that can activate class A orphan receptors GPR176 and GPR37. GPR176 was previously found to be enriched in the mouse suprachiasmatic nucleus (SCN) of the hypothalamus, the central pacemaker that controls the circadian rhythm[50,75]. Its protein expression levels oscillate according to the circadian period being higher during the night, and GPR176-deficient mice display a significantly shorter circadian period compared to their wild-type littermates. Further studies indicated that GPR176 is probably not a light signal-related receptor for the SCN; rather, it seems to be involved in determining the intrinsic period of the SCN. Finally, heterologous expression of GPR176 blunted the forskolin-induced accumulation of cAMP suggesting its coupling to heterotrimeric $G_{i/o/z}$ proteins[50]. Overall, these findings indicate that GPR176 is involved in the suppression of cAMP production in the SCN during nighttime, which serves as the molecular mechanism for its regulation of the circadian period[76]. GPR176 roles outside the central nervous system have also been described[77]; however, no endogenous or synthetic ligands capable of activating GPR176 have been identified yet. With G_zESTY enabling the detection of GPR176 endogenous ligand in the mouse brain, we will be able to perform further studies leading to its isolation. GPR37 is a brain-enriched orphan GPCR with some of the highest transcript levels among all GPCRs[78]. Despite its well-studied involvement in Parkinson's disease, inflammatory responses, and pain, the identity of its endogenous ligand remains a topic of debate[51,79–81]. Early studies proposed prosaptide, a fragment of the secreted neuroprotective and glioprotective factor prosaposin, as the endogenous ligand for GPR37[52]. The identity of this ligand-receptor pair was supported by the fact that prosaptide stimulation of cells transfected with GPR37 induced ERK phosphorylation in a PTX-sensitive manner suggesting coupling to $G_{i/o}$ proteins[52]. Moreover, ^{35}S-GTPγS binding assays and inhibition of forskolin-induced cAMP accumulation all pointed at prosaptide as the endogenous ligand for GPR37[52]. GPR37 activation by prosaptide was later confirmed by measuring a PTX-sensitive intracellular calcium mobilization in GPR37 transfected HEK293 cells[82]. In the same study, activation by neuroprotectin D1 was also observed. Studies in astrocytes also detected GPR37 activation by prosaptide[83]. However, the claim that prosaposin and prosaptide are the endogenous ligands for GPR37 was later challenged by reports demonstrating that GPR37 shows high constitutive activity and that prosaptide treatments were ineffective[51]. Consequently, the prosaptide/GPR37 pairing has yet to be approved by the International Union of Basic and Clinical Pharmacology (IUPHAR) Nomenclature Committee. Given that multiple endogenous ligands can activate the same receptor[8], the pursuit of identifying GPR37 ligands detected using G_zESTY is a valuable endeavor.

Methods

Ethics statement

Procedures involving mice strictly followed NIH guidelines and were approved by the University Committee on Animal Resources (UCAR) at the University of Rochester, animal protocol number UCAR-2019-027.

Cell cultures and transfections

HEK293T/17 cells were purchased from American Type Culture Collection (ATCC) and cultured at 37 °C and 5% CO_2 in Dulbecco's Modified Eagle's Medium (DMEM; Gibco, 10567-014) supplemented with 10% fetal bovine serum (FBS; Biowest, S1520), Minimum Eagle's Medium (MEM) non-essential amino acids (Gibco, 11140-050), sodium pyruvate (Gibco, 11360-070), GlutaMAX (Gibco, 35050-061), and antibiotics (100 units/ml penicillin and 100 μg/ml streptomycin; Gibco, 15140-122). 2×10^6 cells/well were seeded in 6-well plates in 1.5 mL of medium without antibiotics and with 10% dialyzed FBS (Biowest, #S181D). After 4 h, cells were transfected using linear 25 kDa polyethylenimine (PEI) (Polysciences; 23966) at a 1:3 ratio between total μg of DNA plasmid (2.5 μg) and μl of PEI (7.5 μl, 1 mg/ml). A pcDNA3.1 empty vector was used to normalize the amount of transfected DNA. Charcoal-stripped FBS (347G18-CS) and dialyzed FBS (347G18-D) were purchased from Biowest. Cells were routinely monitored for possible mycoplasma contamination. For western blot analysis, 2×10^6 cells/well were plated in each well of a 6-well plate and transfected with the optimized multi plasmids ratio with FLAG-D2R, or with the all-in-one plasmid encoding for G_zESTY and FLAG-D2R. Cells transfected only with pcDNA3.1 served as a specificity control for anti-FLAG antibodies.

DNA constructs and cloning

Plasmids encoding Dopamine D2 Receptor (D2R), GABAB receptor subunits (GABBR1 and GABBR2), α2-adrenergic receptor 2A (ADRA2A), μ-opioid receptor (MOR), δ-opioid receptor (DOR), κ-opioid receptor (KOR) α2-adrenergic receptor 2B (ADRA2B), α2-adrenergic receptor 2C (ADRA2C), serotonin receptor 1B (5-HT1B), masGRK3CT-Nluc, PTX-S1, and $G\alpha_{oA}$ were generous gifts from Dr. Kirill Martemyanov (UF Scripps Institute, FL). $G\beta_1$-Venus$^{156\text{-}239}$ and $G\gamma_2$-Venus$^{1\text{-}155}$ were generous gifts from Dr. Nevin Lambert (Augusta University, GA)[22]. Codon-

optimized coding sequences of the following receptors were a kind gift from Dr. Bryan Roth (University of North Carolina, NC; Addgene kit no. 1000000068)[31] and were used for subcloning into pcDNA3.1 plasmids removing V2-tail, TEV site, and tTA sequences: follicle-stimulating hormone receptor (FSHR), cannabinoid receptor 1 (CB1R), cannabinoid receptor 2 (CB2R), sphingosine-1 phosphate receptor 1 (S1PR1), lysophosphatidic acid 2 receptor (LPAR2), somatostatin receptor 1 (SSTR1), neuropeptide FF receptor 1 (NPFFR1), free fatty acid receptor 3 (FFA3R), galanin 1 receptor (GALR1), formyl peptide receptor 1 (FPR1), hydroxycarboxylic acid receptor 2 (HCAR2), neuropeptide Y receptor Y1 (NPYR1), protease-activated receptor 1 (PAR1), protease-activated receptor 2 (PAR2), histamine receptor H3 (HRH3), dopamine D1 receptor (D1R), dopamine D3 receptor (D3R), adenosine A2B receptor (ADORA2B), parathyroid hormone 1 receptor (PTH1R), melanocortin 4 receptor (MC4R), calcitonin-like receptor (CLR), serotonin receptor 2A receptor (5-HT2AR), GPR55, and muscarinic receptor 3 (M3R). Plasmids encoding the cAMP sensor (pGloSensor™-22F) and CRE-Nluc reporter were purchased from Promega. pFL-tk encoding firefly luciferase under the control of constitutively active thymidine kinase promoter was used as a normalizer for reporter assays. The plasmids encoding the following G_s-derived chimeras were a kind gift from Dr. Robert Lucas (University of Manchester, UK)[27]: GsGz (Addgene plasmid #109355), GsGoB (Cys) (Addgene plasmid #109375), GsGi1/2 (Cys) (Addgene plasmid #109373). pOZITX-S1 was a kind gift from Jonathan Javitch (Addgene plasmid #184925). All constructs were verified by Sanger sequencing.

A modular plasmid system was used to assemble the components of G_zESTY into single multicomponent plasmids. Five insert shuttle plasmids (P1-P5) and a destination plasmid were constructed with matching homology regions for Gibson assembly flanking an insert sequence. For assembly, the shuttle plasmids and destination plasmid were digested with the Type IIS restriction enzyme CspCI, which possesses a relatively rare 7-bp recognition sequence. As CspCI is a type IIS restriction sequence, it cleaves outside of its recognition sequence, allowing for generation of DNA fragments containing unique ends for homology-directed assembly (i.e. Gibson assembly). P1 contained a short CMV promoter (lacks CspCI site found in conventional CMV promoter) driving expression of GloSensor-22F, P2 contained a short ubiquitin C promoter (UbC) driving expression of PTX-S1, P3 contained an ampicillin selection marker and a short CMV promoter driving expression of the receptor of interest, P4 was generally a blank insert except for the GABAB receptor for which P4 contained a short CMV promoter driving expression of the GABAB receptor subunit 2 (with P3 containing subunit 1), and P5 contained a UbC promoter driving expression of the GsGz chimera. To generate plasmids only containing some of these inserts of interest, blank inserts were used for any of P1-P5 containing G_zESTY components not required. The destination plasmid was a pUC57-Kan containing the homologous sequences for Gibson assembly of the inserts. Of note, a plasmid with an alternate resistance marker to AmpR was used as this allows for selection of the final assembled clone without any carry-through of undigested insert plasmids. The CspCI digest contained 110 fmol of each insert plasmid (~375 ng for a 5 kb insert plasmid), 37.5 fmol of the destination plasmid (~125 ng for a 5 kb destination plasmid), 5 μL rCutSmart buffer (NEB), and 1 μL CspCI (5000 units/mL; NEB) in a 50 μL reaction, incubated at 37 °C for 1 h, and heat-inactivated at 65 °C for 20 min. For the Gibson assembly, 5 μL of the CspCI digest was mixed with 5 μL of NEBuilder HiFi DNA Assembly Master Mix (NEB), incubated at 50 °C for 15 min. For transformation of the assembled plasmid, 1.5 μL of the Gibson assembly mix was transformed into either NEB 5-alpha Competent *E. coli* (NEB) or NEB 10-beta Electrocompetent *E. coli* (NEB) and plated on selective LB agar containing both kanamycin (selects for destination plasmid backbone) and ampicillin (selects for P3 insert). G_zESTY all-in-one construct plasmids can be propagated in NEB 5-alpha E. coli in LB media supplemented with proper antibiotics at 37 °C, although care should be taken not to grow cultures longer than 16 h to prevent possible recombination of the plasmids. All plasmids used in this study were verified by whole-plasmid sequencing, performed by Plasmidsaurus using Oxford Nanopore Technology with custom analysis and annotation (Plasmidsaurus Inc). Each plasmid prep was verified to possess the expected DNA sequence and that the read length histogram contained a single plasmid species of the correct size. The expected sizes for the G_zESTY plasmids are as follows, 2-in-one (10,879 bp), 3-in-one (21,933 bp), and 4-in-one D2R (14,638 bp).

Chemicals

The following chemicals were purchased: clonidine (Tocris), dopamine (Tocris), GABA (Tocris), serotonin (Tocris), 1-oleoyl lysophosphatidic acid (Tocris), DAMGO (MedChemExpress), TFLLR (MedChemExpress), human PAR-2 (1-6, SLIGKV) (MedChemExpress), human galanin (1–30) (MedChemExpress), IBMX (MedChemExpress), SEW2871 (MedChemExpress), somatostatin-14 (Cpc Scientific), human neuropeptide Y (13-36) (Cpc Scientific), neuropeptide FF (Thermo Scientific Chemicals), MK-6892 (MedChemExpress), 2-arachidonoyl glycerol (Cayman Chemicals), N-Formyl-Met-Leu-Phe (R&D systems), SNC80 (Adipogen), isobutyric acid (TCI chemicals), salvinorin A (ChromaDex Inc.), morphine (Mallinckrodt Chemical Company), human β-endorphin (Sigma-Aldrich), teriparatide (MedChemExpress), NDP-α-MSH (Phoenix Pharmaceuticals), AB-MECA (MedChemExpress), quinpirole (Tocris), calcitonin gene-related peptide (CGRP) (AnaSpec), AM-251 (Tocris; #1117), carbachol (Tocris; #2810), L-741626 (Tocris; #1003), RS-79948 (Tocris; #0987), saclofen (MCE; #HY-100813), and naloxone (Tocris; #0599). The SCREEN-WELL® Orphan ligand library was purchased from Enzo Life Sciences (BML-2825).

cAMP measurements using G_zESTY

HEK293T/17 cells were transfected as described above with pGloSensor™-22F cAMP plasmid (Promega) and indicated plasmids for mammalian expression of GPCRs, PTX-S1 (or OZITX-S1), and Gs-based chimeras (GsGo, GsGi, or GsGz). 18 hours post-transfection, cells were mechanically detached using a gentle stream of PBS, centrifuged at 500 × *g* for 5 min, and resuspended in 300 μl of PBS containing 0.5 mM $MgCl_2$ and 0.1% glucose. 40 μl of the cell suspension, containing approximately 250,000 cells, were transferred to each well of 96-well flat-bottomed white plates (Greiner Bio-One). D-Luciferin potassium salt (Gold Bio; #DLUCK100) was dissolved in HEPES buffer 10 mM pH 7.4 to obtain a 50x stock at 30 mg/mL. 10 μL of 5X D-luciferin (3 mg/mL) solution were added to the cells. Cells were then incubated at 37 °C and 5% CO_2 for 1 h and then equilibrated in the plate reader at 28 °C, until stable baseline values were reached (~15 min). The luminescence signal was monitored approximately every 30 s using a POLARstar Omega microplate reader (BMG Labtech).

In assays performed on coated 96 well plates, cells were transfected in 6-well plates. The day after transfection, the media was removed, and cells were gently washed with PBS once and briefly trypsinized with 100 μL of trypsin. Trypsinization was blocked by the addition of 900 μL of transfection media containing 10% FBS, cells were counted and seeded at 6.5×10^4 cells/well on a sterile white 96-well plate coated with poly-D-lysine. Cells were then incubated overnight at 37 °C and 5% CO_2. 24 h later, media in each well was replaced with 40 μL of PBS containing 0.5 mM $MgCl_2$, 0.1% glucose, and 10 μL of 5X D-Luciferin, and then incubated for 1 h at 37 °C. The 96-well plate was moved into the plate reader, equilibrated at 28 °C until stable luminescence values were obtained and finally treated according to the experiment setup.

G protein nanoBRET assay

GPCR activation in live cells was measured as BRET signal between Venus-Gβ1γ2 and masGRK3CT-Nluc performed as described previously[23]. 2.5 μg of total DNA was transfected according to the

following ratio: 0.21 μg of Gβ1-Venus(156-239); 0.21 μg of Gγ2-Venus(1-155); 0.013 μg of masGRK3CT-Nluc; 0.83 μg of Gα proteins; and 0.21 μg of receptor. 0.21 μg of RIC8A (for Gq and G15) or RIC8B (for Gs) were also co-transfected. Empty vector pcDNA3.1 was used to normalize the amount of transfected DNA. 18 h after transfection, HEK293T/17 cells were washed once with PBS. For GPR55 transfected cells, wells were serum-starved in optiMEM 4 h before testing. Cells were then mechanically harvested using a gentle stream of PBS, centrifuged at 500 × *g* for 5 min, and resuspended in 500 μl of PBS containing 0.5 mM $MgCl_2$ and 0.1% glucose. 25 μl of resuspend cells, containing approximately 100'000 cells, were distributed in 96-well flat-bottomed white microplates (Greiner Bio-One). The Nluc substrate, furimazine (N1120; Promega) was used according to the manufacturer's instructions. Luminescence was quantified at room temperature using a POLARstar Omega microplate reader (BMG Labtech). BRET signal was determined by calculating the ratio of the light emitted by Venus-Gβ1γ2 (collected using the emission filter 535/30) to the light emitted by masGRK3CT-Nluc (475/30). The average baseline value (basal BRET ratio) was recorded for 2 min prior application of 2x agonist previously dissolved in BRET buffer. Recordings continued for 5 min after agonist application. Average of the baseline BRET ratio was subtracted from maximal BRET ratio obtained upon agonist application to obtain the ΔBRET ratio for each Gα protein.

CRE luciferase reporter assay

HEK293T/17 cells were plated at a density of 1×10^6 cells/well in 6-well plates in an antibiotic-free medium and transfected as described above. 2.5 μg of total DNA was transfected according to the following ratio: 0.10 μg of pFL-tk plasmid expressing firefly luciferase under control of the constitutive thymidine kinase promoter; 0.21 μg of CRE-Nluc luciferase reporter; 1.98 μg of GPCR; and only in experiments screening $G_{i/o}$ activation, 0.21 μg of GsGi1 chimera. pcDNA3.1 was used to normalize the amount of transfected DNA. Cells were incubated overnight and then serum-starved in Opti-MEM for 4 h before collection. Transfected cells were harvested using a gentle stream of PBS, centrifuged for 5 minutes at 500 × *g*, and resuspended in 150 μl of PBS containing 0.5 mM $MgCl_2$ and 0.1% glucose. 30 μl of cells, containing approximately 200,000 cells, were incubated in 96-well flat-bottomed white microplates (Greiner Bio-One) with 30 μl of luciferase substrate according to manufacturers' instructions: furimazine (Promega NanoGlo; N1120) for Nluc, and D-luciferin (Promega BrightGlo; E2610) for firefly luciferase. Luciferase levels were quantified using a POLARstar Omega microplate reader (BMG Labtech). Firefly luciferase expression was used to normalize the signal and compensate for variability due to transfection efficiency and number of cells.

cAMP inhibition assay

HEK293T/17 cells were transfected as described above with pGloSensor™-22F cAMP plasmid (Promega) and plasmids for mammalian expression of indicated GPCRs. The following day, cells were collected in PBS, centrifuged at 500 × *g* for 5 min at room temperature, and the supernatant was discarded. The cell pellet was resuspended in 300 μL of BRET buffer. 40 μL of the resuspended cells (approximately 250,000 cells) was plated into each well of a white 96-well plate, followed by the addition of 10 μL of D-luciferin substrate. The plate was then placed in the POLARstar Omega plate reader, where it was equilibrated at 28 °C until a stable baseline value was recorded. After baseline stabilization, measurements were paused, and the cells were treated with the respective compounds or vehicle for 30 s before adding 10 μM forskolin. Measurement recording resumed thereafter and continued for 20 min. A fold change (FC) was calculated for each sample, similar to the approach used for G_zESTY, by dividing the maximum relative light units (RLU) obtained after forskolin application by the average baseline RLU. For the quinpirole concentration-response curve, the FC for samples treated with the vehicle was averaged and considered 100% of forskolin-induced cAMP levels. The FC of all other samples was then normalized to the vehicle control FC average and expressed as a percentage of cAMP inhibition. In brain extract experiments, forskolin was co-applied with the extract, with or without a specific receptor antagonist. Antagonists were used at a final concentration of 10 μM. A FC was calculated for each sample and normalized to the FC observed with the brain extract in the presence of the respective antagonist. Results from pcDNA3.1-transfected cells were averaged and used for the normalization of the respective receptor.

Determination of components in mouse brain extracts

Levels of dopamine and norepinephrine were quantified using ELISA assays (#KA1887 and #KA3836; Abnova) from 10 μL of sample according to manufacturer's instructions. Unsaturated fatty acids were quantified using a colorimetric Lipid Quantification Kit (#STA-613; Cell Biolabs) according to manufacturer's protocols. 260/280 and 260/230 absorbance ratios were determined using a Nanodrop (Thermofisher Scientific). Protein concentration was determined by Pierce 660 nm Protein Assay Reagent (#1861426; Thermofisher Scientific).

Western blot analysis

Rabbit anti-FLAG antibodies were purchased from Genscript (#A00170; 1:1000), mouse anti-GAPDH antibody was purchased from SIGMA (#MAB374; 1:4000). HRP-conjugated secondary antibodies were purchased from Kindle Bioscience and used at 1:1000 dilution. Transfected cells were collected in PBS and centrifuged at 500 × *g* at room temperature. The supernatant was discarded, and the cell pellet lysed in 250 μL of ice-cold lysis buffer (300 mM NaCl, 50 mM Tris-HCl, pH 7.4, 1% Triton X-100, complete protease inhibitor cocktail from Roche Applied Science) by sonication at 30% power for 10 s on ice. The lysates were centrifuged at 14,000 × *g* for 10 minutes at 4 °C. The supernatant was collected, and the protein concentration was determined using the Pierce 660 nm Protein Assay (Thermofisher Scientific). An equal mass of protein samples was diluted with 4× SDS sample buffer and analyzed by SDS-polyacrylamide gel electrophoresis (SDS-PAGE).

Mice

C57BL/6J mice were housed in a temperature and humidity-controlled room in the vivarium of the University of Rochester on a 12:12-h light/dark cycle (lights off at 18:00 h) provided with food and water ad libitum. Male and female adult mice were used for the experiments. Mice were sacrificed by cervical dislocation, the head was removed and placed immediately in a microwave at maximum power for 10 s to block protease activity[49] (this step was omitted to obtain non-microwaved brain extracts). One brain was removed and immediately homogenized in a glass-glass Dounce homogenizer with 4 mL of PBS. The obtained brain suspension is referred to as the "homogenate fraction". The homogenate fraction was then sonicated once on ice for 10 s at 30% power and centrifuged for 10 min at 14,000 × *g* at 4 °C, obtaining a "supernatant fraction" and a pellet. Each pellet was resuspended in 1.5 mL of PBS and sonicated once on ice for 10 s at 30% power to allow complete resuspension, resulting in the "pellet fraction". 50 μL of each fraction was then applied to the transfected cells. Brains were collected between 2 and 4 PM. All procedures were pre-approved and carried out following the University Committee on Animal Resources (UCAR, protocol number UCAR-2019-027) at the University of Rochester. Bovine pituitary extract was purchased from MP biologicals (cat#2850450).

Statistical analysis

Statistical analysis was performed using GraphPad Prism 9 software. The number of replicates and type of statistical analysis used are described in each figure legend.

Reporting summary

Further information on research design is available in the Nature Portfolio Reporting Summary linked to this article.

Data availability

Raw data that support the findings of this study are available in Figshare with the identifier 26513233. Any additional information required to reanalyze the data reported in this paper is available from the corresponding author upon request.

References

1. Insel, P. A. et al. GPCRomics: an approach to discover GPCR drug targets. *Trends Pharm. Sci.* **40**, 378–387 (2019).
2. Sriram, K. & Insel, P. A. G protein-coupled receptors as targets for approved drugs: how many targets and how many drugs? *Mol. Pharm.* **93**, 251–258 (2018).
3. Gomes, I. et al. GPR171 is a hypothalamic G protein-coupled receptor for BigLEN, a neuropeptide involved in feeding. *Proc. Natl Acad. Sci. USA* **110**, 16211–16216 (2013).
4. Gomes, I. et al. Identification of GPR83 as the receptor for the neuroendocrine peptide PEN. *Sci. Sig* **9**, ra43 (2016).
5. Yosten, G. L. et al. GPR160 de-orphanization reveals critical roles in neuropathic pain in rodents. *J. Clin. Invest.* **130**, 2587–2592 (2020).
6. Franchini, L. & Orlandi, C. Probing the orphan receptors: tools and directions. *Prog. Mol. Biol. Transl. Sci.* **195**, 47–76 (2023).
7. De Giovanni, M. et al. GPR35 promotes neutrophil recruitment in response to serotonin metabolite 5-HIAA. *Cell* **185**, 815–830 e819 (2022).
8. Foster, S. R. et al. Discovery of human signaling systems: pairing peptides to G protein-coupled receptors. *Cell* **179**, 895–908 e821 (2019).
9. Liberles, S. D. & Buck, L. B. A second class of chemosensory receptors in the olfactory epithelium. *Nature* **442**, 645–650 (2006).
10. Isberg, V. et al. Computer-aided discovery of aromatic l-alpha-amino acids as agonists of the orphan G protein-coupled receptor GPR139. *J. Chem. Inf. Model* **54**, 1553–1557 (2014).
11. Southern, C. et al. Screening beta-arrestin recruitment for the identification of natural ligands for orphan G-protein-coupled receptors. *J. Biomol. Screen* **18**, 599–609 (2013).
12. Graaf, C. et al. Glucagon-like peptide-1 and its class B G protein-coupled receptors: a long march to therapeutic successes. *Pharmacol. Rev.* **68**, 954–1013 (2016).
13. Goke, R. & Conlon, J. M. Receptors for glucagon-like peptide-1(7-36) amide on rat insulinoma-derived cells. *J. Endocrinol.* **116**, 357–362 (1988).
14. Shimizu, I., Hirota, M., Ohboshi, C. & Shima, K. Identification and localization of glucagon-like peptide-1 and its receptor in rat brain. *Endocrinology* **121**, 1076–1082 (1987).
15. Thorens, B. Expression cloning of the pancreatic beta cell receptor for the gluco-incretin hormone glucagon-like peptide 1. *Proc. Natl Acad. Sci. USA* **89**, 8641–8645 (1992).
16. Graziano, M. P., Hey, P. J., Borkowski, D., Chicchi, G. G. & Strader, C. D. Cloning and functional expression of a human glucagon-like peptide-1 receptor. *Biochem. Biophys. Res. Commun.* **196**, 141–146 (1993).
17. Dillon, J. S. et al. Cloning and functional expression of the human glucagon-like peptide-1 (GLP-1) receptor. *Endocrinology* **133**, 1907–1910 (1993).
18. Knudsen, L. B. & Lau, J. The discovery and development of liraglutide and semaglutide. *Front. Endocrinol.* **10**, 155 (2019).
19. ElSayed, N. A. et al. 9. Pharmacologic approaches to glycemic treatment: standards of care in diabetes-2023. *Diab. Care* **46**, S140–S157 (2023).
20. FDA. *FDA approves new drug treatment for chronic weight management, first since 2014* (FDA, 2021).
21. Olsen, R. H. J. et al. TRUPATH, an open-source biosensor platform for interrogating the GPCR transducerome. *Nat. Chem. Biol.* **16**, 841–849 (2020).
22. Hollins, B., Kuravi, S., Digby, G. J. & Lambert, N. A. The c-terminus of GRK3 indicates rapid dissociation of G protein heterotrimers. *Cell Signal* **21**, 1015–1021 (2009).
23. Masuho, I. et al. Distinct profiles of functional discrimination among G proteins determine the actions of G protein-coupled receptors. *Sci. Signal* **8**, ra123 (2015).
24. Jang, W., Lu, S., Xu, X., Wu, G. & Lambert, N. A. The role of G protein conformation in receptor-G protein selectivity. *Nat. Chem. Biol.* https://doi.org/10.1038/s41589-022-01231-z (2023).
25. Cao, Y., Namkung, Y. & Laporte, S. A. Methods to monitor the trafficking of beta-Arrestin/G protein-coupled receptor complexes using enhanced bystander BRET. *Methods Mol. Biol.* **1957**, 59–68 (2019).
26. Namkung, Y. et al. Monitoring G protein-coupled receptor and beta-arrestin trafficking in live cells using enhanced bystander BRET. *Nat. Commun.* **7**, 12178 (2016).
27. Ballister, E. R., Rodgers, J., Martial, F. & Lucas, R. J. A live cell assay of GPCR coupling allows identification of optogenetic tools for controlling Go and Gi signaling. *BMC Biol.* **16**, 10 (2018).
28. Binkowski, B. F. et al. A luminescent biosensor with increased dynamic range for intracellular cAMP. *ACS Chem. Biol.* **6**, 1193–1197 (2011).
29. Jiang, L. I. et al. Use of a cAMP BRET sensor to characterize a novel regulation of cAMP by the sphingosine 1-phosphate/G13 pathway. *J. Biol. Chem.* **282**, 10576–10584 (2007).
30. Ma, Q., Ye, L., Liu, H., Shi, Y. & Zhou, N. An overview of Ca(2+) mobilization assays in GPCR drug discovery. *Expert Opin. Drug Discov.* **12**, 511–523 (2017).
31. Kroeze, W. K. et al. PRESTO-Tango as an open-source resource for interrogation of the druggable human GPCRome. *Nat. Struct. Mol. Biol.* **22**, 362–369 (2015).
32. Cheng, Z. et al. Luciferase reporter assay system for deciphering GPCR pathways. *Curr. Chem. Genomics* **4**, 84–91 (2010).
33. Fang, Y., Li, G. & Ferrie, A. M. Non-invasive optical biosensor for assaying endogenous G protein-coupled receptors in adherent cells. *J. Pharm. Toxicol. Methods* **55**, 314–322 (2007).
34. Verdonk, E. et al. Cellular dielectric spectroscopy: a label-free comprehensive platform for functional evaluation of endogenous receptors. *Assay. Drug Dev. Technol.* **4**, 609–619 (2006).
35. Watkins, L. R. & Orlandi, C. In vitro profiling of orphan G protein coupled receptor (GPCR) constitutive activity. *Br. J. Pharm.* **178**, 2963–2975 (2021).
36. Conklin, B. R., Farfel, Z., Lustig, K. D., Julius, D. & Bourne, H. R. Substitution of three amino acids switches receptor specificity of Gq alpha to that of Gi alpha. *Nature* **363**, 274–276 (1993).
37. Inoue, A. et al. Illuminating G-protein-coupling selectivity of GPCRs. *Cell* **177**, 1933–1947.e1925 (2019).
38. Barnett, M. E., Knapp, B. I. & Bidlack, J. M. Unique pharmacological properties of the kappa opioid receptor signaling through Galphaz as shown with bioluminescence resonance energy tranfer. *Mol. Pharm.* **98**, 462–474 (2020).
39. Keen, A. C. et al. OZITX, a pertussis toxin-like protein for occluding inhibitory G protein signalling including Galpha(z). *Commun. Biol.* **5**, 256 (2022).
40. Dunn, H. A., Orlandi, C. & Martemyanov, K. A. Beyond the Ligand: Extracellular and Transcellular G Protein-Coupled Receptor Complexes in Physiology and Pharmacology. *Pharm. Rev.* **71**, 503–519 (2019).
41. Pandy-Szekeres, G. et al. The G protein database, GproteinDb. *Nucleic Acids Res.* **50**, D518–D525 (2022).
42. Pandy-Szekeres, G. et al. GproteinDb in 2024: new G protein-GPCR couplings, AlphaFold2-multimer models and interface interactions. *Nucleic Acids Res.* **52**, D466–D475 (2024).

43. Devane, W. A. et al. Isolation and structure of a brain constituent that binds to the cannabinoid receptor. *Science* **258**, 1946–1949 (1992).
44. Kojima, M. et al. Ghrelin is a growth-hormone-releasing acylated peptide from stomach. *Nature* **402**, 656–660 (1999).
45. Staleva, L. & Orlow, S. J. Ocular albinism 1 protein: trafficking and function when expressed in Saccharomyces cerevisiae. *Exp. Eye Res.* **82**, 311–318 (2006).
46. Tatemoto, K. et al. Isolation and characterization of a novel endogenous peptide ligand for the human APJ receptor. *Biochem. Biophys. Res. Commun.* **251**, 471–476 (1998).
47. Mechoulam, R. et al. Identification of an endogenous 2-monoglyceride, present in canine gut, that binds to cannabinoid receptors. *Biochem. Pharm.* **50**, 83–90 (1995).
48. Franchini, L. & Orlandi, C. Deorphanization of G Protein Coupled Receptors (GPCRs): a historical perspective. *Mol. Pharmacol*. https://doi.org/10.1124/molpharm.124.000900 (2024).
49. Che, F. Y., Lim, J., Pan, H., Biswas, R. & Fricker, L. D. Quantitative neuropeptidomics of microwave-irradiated mouse brain and pituitary. *Mol. Cell Proteom.* **4**, 1391–1405 (2005).
50. Doi, M. et al. Gpr176 is a Gz-linked orphan G-protein-coupled receptor that sets the pace of circadian behaviour. *Nat. Commun.* **7**, 10583 (2016).
51. Smith, N. J. Drug discovery opportunities at the endothelin B receptor-related orphan G protein-coupled receptors, GPR37 and GPR37L1. *Front. Pharm.* **6**, 275 (2015).
52. Meyer, R. C., Giddens, M. M., Schaefer, S. A. & Hall, R. A. GPR37 and GPR37L1 are receptors for the neuroprotective and glioprotective factors prosaptide and prosaposin. *Proc. Natl Acad. Sci. USA* **110**, 9529–9534 (2013).
53. Burris, K. D. et al. Lack of discrimination by agonists for D2 and D3 dopamine receptors. *Neuropsychopharmacology* **12**, 335–345 (1995).
54. DiRaddo, J. O. et al. A real-time method for measuring cAMP production modulated by Galphai/o-coupled metabotropic glutamate receptors. *J. Pharm. Exp. Ther.* **349**, 373–382 (2014).
55. Huang, S. et al. GPCRs steer G(i) and G(s) selectivity via TM5-TM6 switches as revealed by structures of serotonin receptors. *Mol. Cell* **82**, 2681–2695.e2686 (2022).
56. Kuo, A. et al. In vitro profiling of opioid ligands using the cAMP formation inhibition assay and the beta-arrestin2 recruitment assay: no two ligands have the same profile. *Eur. J. Pharm.* **872**, 172947 (2020).
57. Malcolm, N. J. et al. Mu-opioid receptor selective superagonists produce prolonged respiratory depression. *iScience* **26**, 107121 (2023).
58. Mikheil, D. et al. A bioluminescent and homogeneous assay for monitoring GPCR-mediated cAMP modulation and PDE activity. *Sci. Rep.* **14**, 4440 (2024).
59. Montanez-Miranda, C. et al. Functional assessment of cancer-linked mutations in sensitive regions of regulators of G protein signaling predicted by three-dimensional missense tolerance ratio analysis. *Mol. Pharm.* **103**, 21–37 (2023).
60. Rodriguez, P. et al. Functional profiling of the G protein-coupled receptor C3aR1 reveals ligand-mediated biased agonism. *J. Biol. Chem.* **300**, 105549 (2024).
61. Tse, L. H., Cheung, S. T., Lee, S. & Wong, Y. H. Real-time determination of intracellular cAMP reveals functional coupling of G(s) protein to the melatonin MT(1) receptor. *Int. J. Mol. Sci.* **25**, https://doi.org/10.3390/ijms25052919 (2024).
62. El Daibani, A. et al. Molecular mechanism of biased signaling at the kappa opioid receptor. *Nat. Commun.* **14**, 1338 (2023).
63. Smith, J. S. et al. C-X-C motif chemokine receptor 3 splice variants differentially activate beta-arrestins to regulate downstream signaling pathways. *Mol. Pharm.* **92**, 136–150 (2017).
64. Jeffrey, J. J., Ehlich, L. S. & Roswit, W. T. Serotonin: an inducer of collagenase in myometrial smooth muscle cells. *J. Cell Physiol.* **146**, 399–406 (1991).
65. Sakakibara, S. et al. Identification of lysophosphatidic acid in serum as a factor that promotes epithelial apical junctional complex organization. *J. Biol. Chem.* **298**, 102426 (2022).
66. Saucier, C., Morris, S. J. & Albert, P. R. Endogenous serotonin-2A and -2C receptors in Balb/c-3T3 cells revealed in serotonin-free medium: desensitization and down-regulation by serotonin. *Biochem. Pharm.* **56**, 1347–1357 (1998).
67. Lu, S., Jang, W., Inoue, A. & Lambert, N. A. Constitutive G protein coupling profiles of understudied orphan GPCRs. *PLoS One* **16**, e0247743 (2021).
68. Schihada, H., Shekhani, R. & Schulte, G. Quantitative assessment of constitutive G protein-coupled receptor activity with BRET-based G protein biosensors. *Sci. Signal* **14**, eabf1653 (2021).
69. DiBerto, J. F., Smart, K., Olsen, R. H. J. & Roth, B. L. Agonist and antagonist TRUPATH assays for G protein-coupled receptors. *STAR Protoc.* **3**, 101259 (2022).
70. Alabdali, R., Franchini, L. & Orlandi, C. Galpha protein signaling bias at serotonin 1A receptor. *Mol. Pharm.* **104**, 230–238 (2023).
71. Janicot, R. & Garcia-Marcos, M. Get ready to sharpen your tools: a short guide to heterotrimeric G protein activity biosensors. *Mol. Pharm.* **106**, 129–144 (2024).
72. Masuho, I., Martemyanov, K. A. & Lambert, N. A. Monitoring G protein activation in cells with BRET. *Methods Mol. Biol.* **1335**, 107–113 (2015).
73. Li, C. et al. Enterococcus-derived tyramine hijacks alpha(2A)-adrenergic receptor in intestinal stem cells to exacerbate colitis. *Cell Host Microbe* **32**, 950–963.e958 (2024).
74. Airriess, C. N., Rudling, J. E., Midgley, J. M. & Evans, P. D. Selective inhibition of adenylyl cyclase by octopamine via a human cloned alpha 2A-adrenoceptor. *Br. J. Pharm.* **122**, 191–198 (1997).
75. Yamaguchi, Y. et al. Nmu/Nms/Gpr176 triple-deficient mice show enhanced light-resetting of circadian locomotor activity. *Biol. Pharm. Bull.* **45**, 1172–1179 (2022).
76. Nakagawa, S., Nguyen Pham, K. T., Shao, X. & Doi, M. Time-restricted G-protein signaling pathways via GPR176, G(z), and RGS16 set the pace of the master circadian clock in the suprachiasmatic nucleus. *Int. J. Mol. Sci.* **21**, https://doi.org/10.3390/ijms21145055 (2020).
77. De Smet, V. et al. Orphan receptor GPR176 in hepatic stellate cells exerts a profibrotic role in chronic liver disease. *JHEP Rep.* **6**, 101036 (2024).
78. Fu, W., Franchini, L. & Orlandi, C. Comprehensive spatial profile of the orphan G protein coupled receptor GPRC5B expression in mouse brain. *Front. Neurosci.* **16**, 891544 (2022).
79. Zhang, Q., Bang, S., Chandra, S. & Ji, R. R. Inflammation and Infection in Pain and the Role of GPR37. *Int. J. Mol. Sci.* **23**, https://doi.org/10.3390/ijms232214426 (2022).
80. Meyer, R. C., Giddens, M. M., Coleman, B. M. & Hall, R. A. The protective role of prosaposin and its receptors in the nervous system. *Brain Res.* **1585**, 1–12 (2014).
81. Bolinger, A. A., Frazier, A., La, J. H., Allen, J. A. & Zhou, J. Orphan G protein-coupled receptor GPR37 as an emerging therapeutic target. *ACS Chem. Neurosci.* **14**, 3318–3334 (2023).
82. Bang, S. et al. GPR37 regulates macrophage phagocytosis and resolution of inflammatory pain. *J. Clin. Invest.* **128**, 3568–3582 (2018).
83. Liu, B. et al. Glio- and neuro-protection by prosaposin is mediated by orphan G-protein coupled receptors GPR37L1 and GPR37. *Glia* **66**, 2414–2426 (2018).

Acknowledgements

This work was supported by start-up funding from the Department of Pharmacology and Physiology, University of Rochester School of Medicine and Dentistry to C.O.; Ernest J. Del Monte Institute for Neuroscience Pilot Program, University of Rochester, to C.O.; University Research

Award, University of Rochester to C.O; NIDCD/NIH grant R01DC022104 to C.O.; R01HL153988 to J.D.L.; this work was aided by the GCE4All Biomedical Technology Optimization and Dissemination Center supported by National Institute of General Medical Science grant RM1-GM144227; The Foundation Blanceflor Boncompagni Ludovisi-née Bildt fellowship to L.F.

Author contributions

Experimental investigation and data analysis, L.F., J.J.P., J.D.L. and C.O.; Conceptualization, L.F. and C.O.; writing and editing—original draft preparation, C.O.; All authors have read and agreed to the published version of the manuscript.

Competing interests

The authors declare no competing interests.

Additional information

Supplementary information The online version contains supplementary material available at https://doi.org/10.1038/s41467-025-59850-8.

Correspondence and requests for materials should be addressed to Cesare Orlandi.

Peer review information *Nature Communications* thanks Nicola Smith who co-reviewed with Brendan Wilkinsand the other, anonymous, reviewer(s) for their contribution to the peer review of this work. A peer review file is available.